ELECTROMAGNETIC WAVE PROPAGATION IN A COAXIAL WAVEGUIDE WITH AN ANNULAR MAGNETIZED FERRITE ROD

ISAAC DAVIES, B.E.

Electromagnetic Wave Propagation In A Coaxial Waveguide With An Annular Magnetized Ferrite Rod

By

©Isaac Davies, B. E.

A thesis submitted to the School of Graduate

Studies in partial fulfillment of the

requirements for the degree of

Master of Engineering

Faculty of Engineering and Applied Science

Memorial University of Newfoundland

July 1992

St. John's Newfoundland Canada

ISBN 0-315-78115-7

Abstract

The propagation of electromagnetic waves in a coaxial waveguide loaded with ferrite is studied by using the exact analysis approach. The results of the partially filled ferrite case (radii ratio '$S_o = 0.5$') and the approximately fully filled ferrite case (radii ratio '$S_o = 0.9$') are given for the dipolar modes ($n = \pm 1$). The ferrite used is assumed to be lossless and completely magnetized. A review of the electromagnetic wave propagation in an infinite ferrite medium is presented to point out the various wave propagation characteristics in the parametric space diagrams. In the exact analysis method, the general dispersion relations are derived directly from Maxwell's equations. Initially, the cutoff and resonant frequencies are examined analytically to predict all possible modes. By employing numerical root search technique the complete dispersion characteristics are obtained.

The occuring modes in the different parametric regions are identified and properly classified to provide a better understanding of the basic mode structure in these types of waveguides which are filled with anisotropic materials. Also, the effects of the radii ratio and the dc magnetic field on the various modes are discussed. Finally, some applicational aspects of such waveguides are considered, especially, in the design of phase shifters where the characteristics of the pairs of dominant waveguide modes play an important role.

Acknowledgements

Completion of this research would not have been possible without the help of numerous people. Professor Son Le-Ngoc provided valuable advice, guidance and support throughout my graduate studies. I am extremely grateful for the financial aid provided during the course of my work by NSERC, the School of Graduate Studies and the Faculty of Engineering and Applied Sciences, Memorial University of Newfoundland for which I would like to thank Dr. J. Malpas and Dr. T. R. Chari. A word of praise to my fellow graduate students for their help and advice. Finally, I would like to thank my parents for their years of support, patience and encouragement of which no description in words would suffice.

Contents

List of Figures

List of Tables

List of Symbols

ω	operating frequency.
ω_m	saturation magnetization frequency.
k_o	free-space propagation constant.
k	propagation constant.
n	azimuthal variation number.
v	velocity of light.
q	normalized ferrite column radius.
γ	normalized propagation constant.
ϵ_f	relative dielectric constant of ferrite.
ϵ_1	relative dielectric constant of region 1.
ϵ_3	relative dielectric constant of region 3.
$\underline{\underline{\mu}}$	permeability tensor.
$\eta_{1,2}$	radial wave numbers.
Ω	normalized frequency.
Ω_H	normalized gyromagnetic frequency.
Ω_c	hybrid resonant frequency.
S_o	radii ratio.
H_o	D.C. magnetic field.
$\underline{E}$	normalized electric field vector.

$\underline{H}$	normalized magnetic field vector.
$J_n(x)$	Bessel function of the first kind of order n & argument x.
$N_n(x)$	Bessel function of the second kind of order n & argument x.
$I_n(x)$	modified bessel function of the first kind of order n & argument x.
$K_n(x)$	modified bessel function of the second kind of order n & argument x.
Θ_F	faraday rotation (degrees).
Θ_p	phase shift (degrees).

Chapter 1

INTRODUCTION

Propagation of electromagnetic waves in magnetized ferrites is of great interest to many researchers in the area of microwave devices. When a ferrite is magnetized with a constant magnetic field, its relative permeability is no longer constant but a tensor quantity (tensor permeability) and these ferrites possess non-reciprocal properties. In this thesis an analytical study of the propagation of electromagnetic waves in a coaxial waveguide partially filled with ferrite is considered. One of the main reasons in choosing a coaxial waveguide over a circular one for this study is to reduce the size of the component package which gives an added advantage in many of the applications and also for operating over wide frequency ranges. A lot of microwave ferrite devices have been developed in the past few decades, to name a few; phase shifters, isolators, circulators, gyrators etc. Thus, results obtained from this study can have potential applications in the above mentioned microwave ferrite devices.

1.1 Problem statement

The coaxial waveguide under study has an inner radius 'a' and an outer radius 'd'. A ferrite coaxial tube of inner radius 'b' and outer radius 'c' is enclosed such that $a \leq b \leq c \leq d$. Dielectric materials exist on both its sides i.e. for $a < r < b$

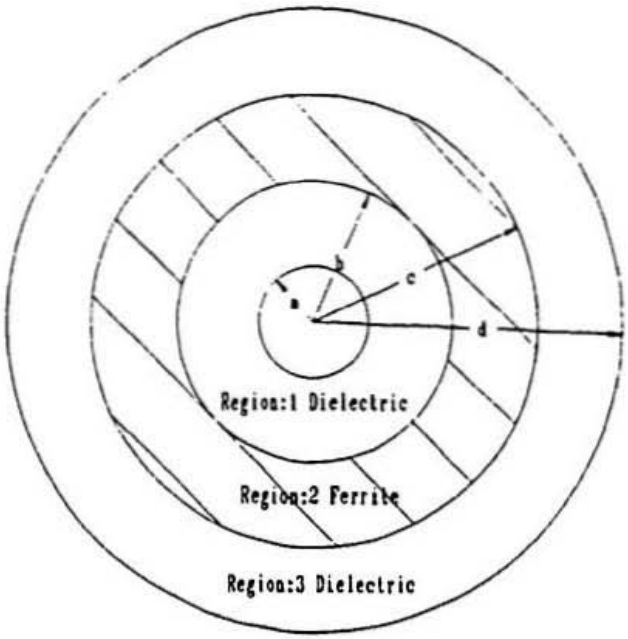

Figure 1.1: Cross-section of a partially loaded ferrite coaxial waveguide

and $c < r < d$ where 'r' is the radial distance in the cylindrical co-ordinates. The configuration of the problem is illustrated in Figure 1.1. As can be seen from the figure, there are three distinct regions namely: Region 1- Dielectric ; Region 2- Ferrite ; Region 3- Dielectric. The dielectric in region 1 is used to support the ferrite tube. Due to the generality of this configuration, the approximately fully filled case is achieved by bringing radius 'b' close to 'a' and radius 'c' close to 'd'. The ferrite used is assumed to be lossless and completely magnetized along the axis by a uniform magnetic field H_o. It becomes an anisotropic magnetic material and exhibits tensor permeability of the following form (Collin, 1966):

$$\underline{\underline{\mu}} = \begin{bmatrix} \mu_1 & j\mu_2 & 0 \\ -j\mu_2 & \mu_1 & 0 \\ 0 & 0 & 1 \end{bmatrix} \tag{1.1}$$

where μ_1 and μ_2 denote the permeability constants in region 1 and region 2 repectively. In a cylindrical co-ordinate system (r, ϕ, z), the fields are assumed as follows

(Le-Ngoc, 1975):

$$
\begin{aligned}
F(r,\phi,z) &= F(r)exp[j(kz+n\phi-\omega t)] \\
k &\quad \text{phase constant} \\
n &\quad \text{azimuthal variation number} \\
\omega &\quad \text{operating frequency (rad/sec)}
\end{aligned}
\tag{1.2}
$$

Maxwell's equations for a source free medium is given as :

$$\nabla \times \underline{E_1} = -\partial \underline{B_1}/\partial t \tag{1.3}$$

$$\nabla \times \underline{H_1} = \partial \underline{D_1}/\partial t \tag{1.4}$$

where $\underline{E_1}$ and $\underline{H_1}$ represent the unnormalized field vectors. The constituent equations for the ferrite case are given as :

$$\underline{D_1} = \epsilon_o \epsilon_f \underline{E_1} \tag{1.5}$$

$$\underline{B_1} = \mu_o \underline{\underline{\mu}} \underline{H_1} \tag{1.6}$$

where ϵ_f is the relative dielectric constant of the ferrite and $\underline{\underline{\mu}}$ the tensor permeability which is also represented as follows (Le-Ngoc, 1975):

$$\underline{\underline{\mu}} = \mu_1 \hat{r}\hat{r} + j\mu_2 \hat{r}\hat{\phi} - j\mu_2 \hat{\phi}\hat{r} + \mu_1 \hat{\phi}\hat{\phi} + \mu_3 \hat{z}\hat{z} \tag{1.7}$$

$$\mu_1 = 1 + \Omega_H/(\Omega_H^2 - \Omega^2) \tag{1.8}$$

$$\mu_2 = -\Omega/(\Omega_H^2 - \Omega^2) \tag{1.9}$$

$$\mu_3 = 1 \tag{1.10}$$

where $\Omega(=\omega/\omega_m)$ is the normalised frequency and $\Omega_H(=\omega_H/\omega_m)$ is the normalised gyromagnetic frequency. ω, ω_H and ω_m represent the source, gyromagnetic and

saturation magnetization angular frequencies respectively, (Seshadri, 1973). Generally the theoretical analyses are mainly based on two approaches: the quasi-static approximation and the exact analysis. In the quasi-static analysis the rf electric fields are too small and are neglected, hence the fields are derived from a scalar potential function whereas in the exact analysis the fields are directly derived from the Maxwell's equations. Le-Ngoc (1975) studied the electromagnetic wave propagation in a circular waveguide partially filled with anisotropic materials. He used both methods and showed that the quasi-static method is valid only for propagation constants of large values in predicting possible modes. This merely served to be confirmed by comparison with the modes obtained using exact analysis. Therefore in present study, only the exact analysis approach is considered. The adopted procedure is given as follows:

Initially, the Maxwell's equations are decomposed into transverse and longitudinal components and then by the substitution of the transverse component expressions into the longitudinal ones, a second order partial differential equation in the longitudinal field components is obtained. This is then expressed in terms of two scalar wave functions which are further solved by matrix algebra to yield two partial differential equations in the scalar wave functions, the solution of these equations are individually obtained. By applying the boundary conditions on the various field components, the exact dispersion relations are derived.

1.2 Literature review

In the fifties, theoretical analyses based on two approaches; namely the Quasi-static analysis and the Exact analysis were used to study the propagation of electromagnetic waves in completely filled and partially filled ferrite waveguides. In quasi-static approximation, the phase velocities of the waves are assumed to be

much less than the velocity of light so that the a.c. electric fields can be ignored. The magnetic fields are derived from a scalar function Φ, i.e., $H = \nabla\Phi$. Thus the name magnetostatic approximation came into being (Trivelpiece et al, 1961). Joseph and Schlomann (1961) investigated the mode spectrum of a long circular cylinder of ferromagnetic material (ferrite column in free space). They found that the magnetostatic approximation was justifiable over a large part of the mode spectrum for both axi-symmetric and dipolar modes. Also the surface modes existed only at small wave numbers and that their eigen frequencies being higher than those of the volume modes, were examined. Interestingly, it was seen that the eigen frequencies decreased with increasing wave numbers, because at low wave numbers, the surface charge produces an additional restoring force thereby increasing the frequency.

A study made by Trivelpiece et al. (1961) showed the validity of the quasi-static approximation. They also established the dispersion relations for partially filled, fully filled ferrite waveguides and ferrite rod in space. Magnetostatic approximation was also used by Olson et al. (1967) to categorize surface and volume modes. Using this approximation, Masuda et al. (1971) studied the azimuthally dependent magnetostatic modes for both, a hollow ferrite pipe enclosed in a cylindrical waveguide and a ferrite rod placed at the center of a round waveguide partially filling the cross-section. The dispersion relations were derived for only $n = 1$ modes in both the cases. Their analysis revealed the presence of dielectric medium to be of great importance in determining the cutoff wave number and upper bound frequency of the magnetostatic surface modes.

Employing the exact analysis method, Kales (1953) formulated the dispersion relationships for both the partially and fully filled waveguides of circular symmetry. His study emphasized on the cutoff frequency. Tomkins (1958) provided quantitative data relating field and energy distributions for several cases in a partially

ferrite filled cylindrical waveguide. In a study by Schott et al. (1967), the transition from the exact solution to the magnetostatic limit was investigated for the ferrite column in free space. Numerical computations were also made and compared with the magnetostatic results. Duputz and Priou (1974) developed a new computing method to solve the dispersion relationship of both partially and fully loaded ferrite circular TE_{11} waveguide mode. Their study based on exact analysis assumed the ferrite to be lossy at frequency of 9.5 GHz. Le-Ngoc et al. (1977) made a study on the propagation of electromagnetic waves in a partially ferrite (magnetized and lossless) filled circular waveguide by using both the quasi-static and exact analyses. Dispersion characteristics were studied in detail for the dipolar modes and the cutoffs and resonances were considered.

Interestingly, a study was made by Mueller and Rosenbaum (1977) on the propagation of electromagnetic waves in an azimuthally magnetized ferrite loaded coaxial Transmission Line. The Bolle and Heller functions, which are directly related to the Bessel and Neumann functions respectively were employed to solve the boundary value problem and the dispersion characteristics of the TE modes for the coaxial waveguide were plotted between normalized frequency and normalized propagation constant. The main application is in digitally controlling the nonreciprocal phase shift by pulsing the electric current in the center conductor of a ferrite loaded coaxial waveguide. Samaddar (1979) has proved that the Bolle and Heller functions reduce to the Bessel and Neumann functions in the absence of dc magnetic field and has provided correct fundamental solutions which can be used to solve any problems in the work done by Mueller and Rosenbaum (1977). Igarashi and Nato (1981) have obtained a formula for the parallel component μ_z (same as μ_3) which is a function of magnetization and not unity for a partially magnetized microwave ferrite. Cylindrical coaxial waveguides which are corrugated, find applications as feeds for reflector antennas. Hence studies relating to corrugated

coaxial waveguide were made by James (1983) with reference to frequency band and bandwidth characteristics. Also the various modes were identified and the radiation properties were studied.

In the paper by Thompson and Rodrigue (1985), the theory of planar anisotropy of ferrite phase shifter applied to millimeter wave frequencies is developed and it was found that the differential phase shift depends on the thickness of the ferrite, the phase shift increases with the increase in the ferrite thickness. These phase shifters are generally made of a ferrite toroid with a core of dielectric. The architecture of reciprocal and non-reciprocal phase shifter and a few other microwave devices employing circular waveguides are well illustrated by Helszajn (1987). Daywitt (1990) has solved the Maxwell's equation for a slightly lossy coaxial transmission line to first order in the normalized surface impedance for principal and symmetric waveguide modes. Dispersion characteristics of a strip dielectric waveguide were derived by Chiang (1991) in order to facilitate the design of the strip waveguide. The literature cited above is by no means exhaustive but lists sources associated with the present work.

1.3 Scope of the thesis

The purpose of present thesis is to study the dispersion characteristics of the dipolar modes ($n = \pm 1$) in a partially ferrite filled coaxial waveguide by using the exact analysis approach. The presence of a coaxial waveguide complicates the analysis because additional boundary conditions are to be solved. The general dispersion relations are obtained by the procedure stated above. The cutoff and resonant frequencies are first examined to predict all possible modes by studying the dispesrion relations at cutoff and resonant conditions. Numerical techniques are employed to solve the dispersion relations. In this study, dispersion curves for

both weak and strong d.c. magnetic fields are obtained. The ferrite used is taken to be lossless and completely magnetized.

1.4 Organization of the thesis

This thesis is divided into five chapters. The first chapter, which is being presented, gives a brief introduction to the problem stated and a detailed literature review. The next chapter, chapter 2, outlines the analysis governing the propagation of electromagnetic waves in an infinite anisotropic ferrite leading to parametric space diagrams. Chapter 3 examines the exact analysis of propagation of EM waves in a coaxial waveguide. Numerical results are given in chapter 4. Finally, some applicational aspects and conclusions are given in chapter 5.

Chapter 2

ELECTROMAGNETIC PROPAGATION IN AN UNBOUNDED MAGNETIZED FERRITE

In order to understand the operation of the ferrite devices, it is important to study the basic nature of microwave propagation in an infinite unbounded ferrite medium (Collin 1966). In this chapter, plane wave propagation in an infinte ferrite medium in presence of a dc magnetic field $\underline{H_o}$ is considered. It can be found that the natural modes of propagation in the direction of the dc magnetic field $\underline{H_o}$ constitute left and right circularly polarised waves possessing different propagation constants as will be seen later in this study.

2.1 Electromagnetic plane wave propagating in an infinite magnetized ferrite

The plane wave solutions for the fields in a homogeneous, lossless and infinite ferrite medium are generally written in the form :

$$\underline{F} = \underline{F_o}\ exp[j(\underline{K}.\underline{r} - \omega t)] \tag{2.1}$$

where $\underline{F_o}$ is a constant vector independent of space and time, $\underline{r}$ being a vector from the origin of the co-ordinate system to the required point of observation and $\underline{K}$ representing the propagation vector.

The normalized field vectors $\underline{E}$ and $\underline{H}$ are given as: $\underline{E} = \sqrt{\epsilon_o}\underline{E_1}$ and $\underline{H} = \sqrt{\mu_o}\underline{H_1}$. Now substituting the plane wave solution (2.1) and the normalized field vectors in the Maxwell's equations (1.3) and (1.4) and then by eliminating the $\underline{E}$ field, an equation for the $\underline{H}$ field is obtained as,

$$\underline{K} \times (\underline{K} \times \underline{H}) + k_o^2 \epsilon_f \underline{\mu} \underline{H} = 0 \tag{2.2}$$

where $k_o = \omega/v$ is the propagation constant in free space, v denoting the velocity of light. The matrix form representation of this equation is given below,

$$\begin{bmatrix} k_o^2\epsilon_f\mu_1 - k_z^2 & jk_o^2\epsilon_f\mu_2 & k_\perp k_z \\ -jk_o^2\epsilon_f\mu_2 & k_o^2\epsilon_f\mu_1 - k_\perp^2 - k_z^2 & 0 \\ k_\perp k_z & 0 & k_o^2\epsilon_f - k_\perp^2 \end{bmatrix} \times \begin{bmatrix} H_x \\ H_y \\ H_z \end{bmatrix} = 0 \tag{2.3}$$

where $k_\perp$ and k_z are the transverse and longitudinal propagation constants as shown in Figure 2.1. ϕ being the angle between $\underline{K}$ and $\underline{H_o}$.

The determinant of the matrix has to be zero for non-trivial solutions of $\underline{H}$. Therefore,

$$(k_o^2\epsilon_f - k_\perp^2)[(k_o^2\epsilon_f\mu_1 - k_z^2)(k_o^2\epsilon_f\mu_1 - k_\perp^2 - k_z^2) - k_o^4\epsilon_f^2\mu_2^2] - k_\perp^2 k_z^2(k_o^2\epsilon_f\mu_1 - k_\perp^2 - k_z^2) = 0 \tag{2.4}$$

The longitudinal and transverse propagation constants are normalized as $\gamma = k_z/k_o = k/k_o$ and $\eta = k_\perp/k_o$. By doing this, equation (2.4) becomes,

$$\eta^4 + 1/\mu_1[\epsilon_f(\mu_2^2 - \mu_1^2 - \mu_1) + \gamma^2(\mu_1 + 1)]\eta^2 + 1/\mu_1[\epsilon_f(\mu_2 + \mu_1) - \gamma^2][\epsilon_f(\mu_1 - \mu_2) - \gamma^2] = 0 \tag{2.5}$$

This equation (2.5) is then solved to obtain:

$$\eta_{1,2}^2 = [\epsilon_f(1 + 2\Omega_H) - (\gamma^2 - \epsilon_f)(2\Omega_H^2 - 2\Omega^2 + \Omega_H)]/2(\Omega_H^2 + \Omega_H - \Omega^2)$$

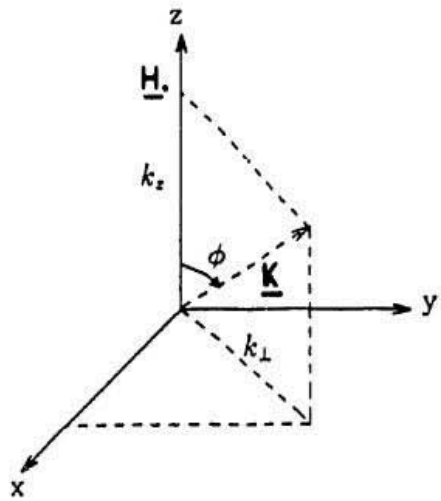

Figure 2.1: Propagation vector diagram

$$\frac{\pm\left[(\Omega_H^2\gamma^2+\epsilon_f(2\Omega^2-\Omega_H^2-\Omega_H))^2-4\Omega^2\epsilon_f^2(\Omega^2-\Omega_H^2-\Omega_H)\right]^{1/2}}{2\Omega_H(\Omega_H^2-\Omega^2+\Omega_H)} \tag{2.6}$$

Although circularly polarized waves are the fundamental modes of propagation, linearly polarized waves seem to occur more often in practice. The detection of a linearly polarized wave in the ferrite results is a measure of the sum of two circularly polarized waves, the propagation constants being different for the two opposite hands of circular polarization thus enabling one hand of the circular polarization to rotate further than the other in a fixed length of the ferrite material. Hence the plane of polarization of the linearly polarized wave that was detected is rotated with respect to the incident wave. This rotation has been referred to as the Faraday rotation (Fuller, 1987). From equation (2.6) it is clear that there exists two kinds of plane waves propagating in an infinite ferrite for a given value of γ, whose transverse propagation constants are given by η_1 and η_2. By introducing the refractive index term ($\zeta = K/k_o$) and ϕ, from equation (2.4), the relation between

ζ and ϕ is established as:

$$\zeta^4[\mu_1 sin^2\phi + cos^2\phi] - \zeta^2[\epsilon_f(\mu_1^2 - \mu_2^2)sin^2\phi + \epsilon_f\mu_1(cos^2\phi + 1)] + (\mu_1^2 - \mu_2^2)\epsilon_f^2 = 0 \quad (2.7)$$

The dispersion equation (2.7) can also be written in another form which is given as follows:

$$tan^2\phi = \frac{-[\zeta^2 - \epsilon_f(\mu_1 - \mu_2)][\zeta^2 - \epsilon_f(\mu_1 + \mu_2)]}{[\mu_1\zeta^2 - \epsilon_f(\mu_1^2 - \mu_2^2)][\zeta^2 - \epsilon_f]} \quad (2.8)$$

The cutoff and resonant frequencies are obtained from equation (2.7) as follows; At cutoff when $\zeta = 0$, we have :

$$\Omega = \Omega_H + 1 \quad (2.9)$$

and at resonance when $\zeta \to \infty$, we have :

$$\Omega^2 - \Omega_H(\Omega_H + sin^2\phi) = 0 \quad (2.10)$$

From these relations, it is seen that the cutoff frquency depends only on Ω_H whereas the resonant frequency not only depends on Ω_H but also on the direction of propagation. The dispersion equation (2.8) is analysed for studying the propagation of waves in the direction specified as will be seen shortly. Also the concept of Faraday rotation plays an important role in this aspect of study.

2.2 Propagation along H_o, $\phi = 0°$

Applying the condition $\phi = 0°$ in equation(2.8), we get two transverse electric and magnetic (TEM) wave solutions:

$$\gamma_1^2 = \epsilon_f[1 + 1/(\Omega_H - \Omega)] \quad (2.11)$$

$$\gamma_2^2 = \epsilon_f[1 + 1/(\Omega_H + \Omega)] \tag{2.12}$$

It can be shown that equation (2.11) which represents a right hand circularly polarised plane wave (RHCP) has a cutoff frequency $\Omega = \Omega_H + 1$ and a resonant frequency $\Omega = \Omega_H$ whereas equation (2.12) which represents a left hand circularly polarised plane wave (LHCP) has neither cutoff nor resonant frequency. The regions of propagation are indicated in the parametric diagram of Figure 2.2. These waves are basically transverse electromagnetic in nature.

2.3 Application to guided waves in ferrites

The behaviour of the transverse propagation constants namely η_1 and η_2 in equation (2.6) are shown in Figure 2.3, where the constant $q = \omega_m d/v = 0.5$ Again referring to Le-Ngoc (1975) the curves are drawn, except that in this case ϵ_f is 12 since the compound taken into consideration is different. These curves divide the $\Omega - \gamma$ plane into four distinct regions as studied by Clarricoats (1961). Schott and Tao (1968) classified the different types of modes on this basis. The four distinct regions are given as follows:

$$\textit{Region I} : \eta_1 \textit{ and } \eta_2 \textit{ are imaginary}$$

$$\textit{Region II} : \eta_1 \textit{ real and } \eta_2 \textit{ imaginary}$$

$$\textit{Region III} : \eta_1 \textit{ imaginary and } \eta_2 \textit{ real}$$

$$\textit{Region IV} : \eta_1 \textit{ and } \eta_2 \textit{ are real}$$

Therefore these curves which classify the different regions are very important and will be made use of in identifying the various modes by exact analysis approach.

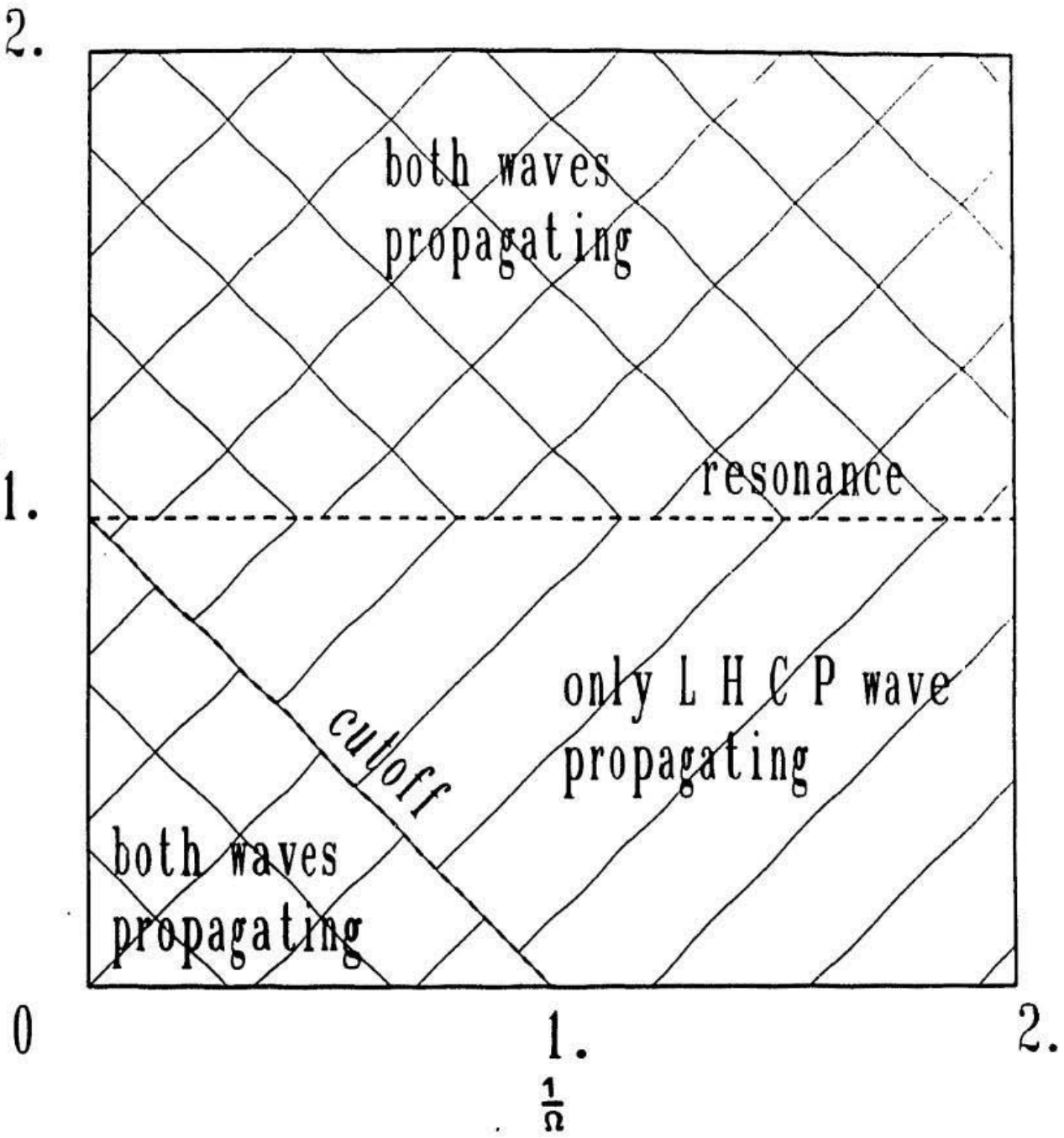

Figure 2.2: Parametric diagram ($\phi = 0°$)

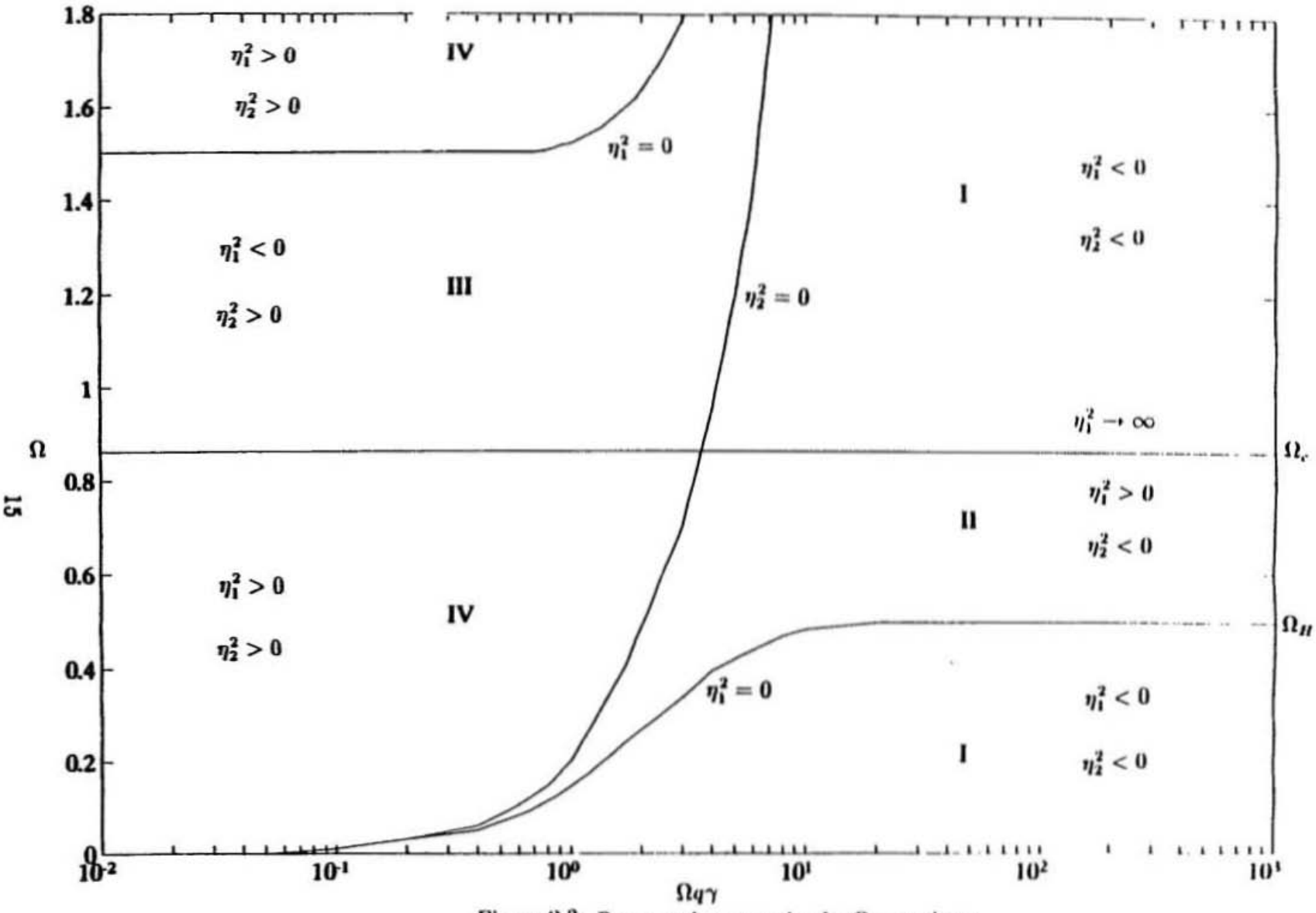

Figure 2.3: Parametric curves in the $\Omega - \gamma$ plane

Chapter 3

ELECTROMAGNETIC WAVE PROPAGATION IN A COAXIAL WAVEGUIDE

3.1 General dispersion relations

The Maxwell's equations (1.3) and (1.4) are considered. By making the following substitutions namely: $\underline{E} = \sqrt{\epsilon_o}\underline{E_1}$, $\underline{H} = \sqrt{\mu_o}\underline{H_1}$ and $k_o = \omega\sqrt{\mu_o c_o}$ in equations (1.3) and (1.4) the Maxwell's equations are now written as:

$$\nabla \times \underline{H} = -jk_o\epsilon_f\underline{E} \tag{3.1}$$

$$\nabla \times \underline{E} = jk_o\underline{\mu}\underline{H} \tag{3.2}$$

In a cylindrical co-ordinate system, the field is given by equation (1.2).

From equations (3.1) and (1.2) we get,

$$\frac{1}{r}\frac{\partial H_z}{\partial \phi} - \frac{\partial H_\phi}{\partial z} = -jk_o\epsilon_f E_r \tag{3.3}$$

$$\frac{\partial H_r}{\partial z} - \frac{\partial H_z}{\partial r} = -jk_o\epsilon_f E_\phi \tag{3.4}$$

$$\frac{1}{r}\frac{\partial (rH_\phi)}{\partial r} - \frac{1}{r}\frac{\partial H_r}{\partial \phi} = -jk_o\epsilon_f E_z \tag{3.5}$$

From equations (3.2) and (1.2) we get,

$$\frac{1}{r}\frac{\partial E_z}{\partial \phi} - \frac{\partial E_\phi}{\partial z} = jk_o[\mu_1 H_r + j\mu_2 H_\phi] \tag{3.6}$$

$$\frac{\partial E_r}{\partial z} - \frac{\partial E_z}{\partial r} = jk_o[-j\mu_2 H_r + \mu_1 H_\phi] \tag{3.7}$$

$$\frac{1}{r}\frac{\partial (rE_\phi)}{\partial r} - \frac{1}{r}\frac{\partial E_r}{\partial \phi} = jk_o H_z \tag{3.8}$$

The transverse electric field components are obtained from equations (3.3) and (3.4) as,

$$E_r = \frac{1}{k_o \epsilon_f}[kH_\phi - \frac{n}{r}H_z] \tag{3.9}$$

and

$$E_\phi = \frac{1}{k_o \epsilon_f}[-kH_r - j\frac{dH_z}{dr}] \tag{3.10}$$

The transverse components are now expressed as a function of the longitudinal component. By the substitution of (3.10) into (3.6), equation (3.6) becomes

$$[\mu_1 \epsilon_f - \gamma^2]H_r + j\mu_2 \epsilon_f H_\phi = \frac{\epsilon_f n}{k_o r}E_z + j\frac{\gamma}{k_o}\frac{dH_z}{dr} \tag{3.11}$$

and by the substitution of (3.9) into (3.7), equation (3.7) becomes

$$j\mu_2 \epsilon_f H_r - [\mu_1 \epsilon_f - \gamma^2]H_\phi = -\frac{1}{k_o}[j\epsilon_f \frac{dE_z}{dr} - \gamma \frac{n}{r}H_z] \tag{3.12}$$

Now using Crammer's rule, the determinant of equations (3.11) and (3.12) is found to be

$$\Delta = [\mu_2 \epsilon_f]^2 - [\mu_1 \epsilon_f - \gamma^2]^2 \tag{3.13}$$

which is assumed to be non-zero. The transverse magnetic components are now written as

$$\begin{aligned} H_r \;=\; & \frac{1}{\Delta}[(-\frac{(\mu_1 \epsilon_f - \gamma^2)}{k_o}\epsilon_f)\frac{n}{r}E_z - \frac{\mu_2 \epsilon_f^2}{k_o}\frac{dE_z}{dr} \\ & - j\frac{\mu_2 \epsilon_f \gamma n}{k_o r}H_z - (\mu_1 \epsilon_f - \gamma^2)\frac{j\gamma}{k_o}\frac{dH_z}{dr}] \end{aligned} \tag{3.14}$$

and

$$\begin{aligned} H_\phi \;=\; & \frac{1}{\Delta}[(-\frac{(\mu_1 \epsilon_f - \gamma^2)}{k_o}j\epsilon_f)\frac{dE_z}{dr} + \frac{\gamma \mu_2 \epsilon_f}{k_o}\frac{dH_z}{dr} \\ & - j\frac{\mu_2 \epsilon_f^2 n}{k_o r}E_z + (\mu_1 \epsilon_f - \gamma^2)\frac{\gamma}{k_o}\frac{n}{r}H_z] \end{aligned} \tag{3.15}$$

Substitution for H_r and H_ϕ into equation (3.5) result in the wave equation:

$$-\frac{j\epsilon_f}{k_o\Delta}(\mu_1\epsilon_f-\gamma^2)\nabla_t^2E_z+\frac{\gamma\mu_2\epsilon_f}{k_o\Delta}\nabla_t^2H_z+jk_o\epsilon_fE_z=0 \tag{3.16}$$

and substituting E_r, E_ϕ and H_r, H_ϕ in equation (3.8) results in the other wave equation:

$$\frac{\gamma\mu_2\epsilon_f}{k_o\Delta}\nabla_t^2E_z+\frac{j}{k_o\epsilon_f}[\frac{\gamma^2(\mu_1\epsilon_f-\gamma^2)}{\Delta}-1]\nabla_t^2H_z-jk_oH_z=0 \tag{3.17}$$

where $\nabla_t^2=\frac{1}{r}\frac{d}{dr}(r\frac{d}{dr})-\frac{n^2}{r^2}$. Equations (3.16) and (3.17) are coupled and they can be decoupled by assuming that $E_z=\Psi$ and $H_z=\alpha\Psi$, α being the proportionality constant. By this assumption, the above equations are written as

$$\nabla_t^2\Psi[-\frac{j}{k_o\Delta}(\mu_1\epsilon_f-\gamma^2)+\frac{\gamma\mu_2\alpha}{k_o\Delta}]+jk_o\Psi=0 \tag{3.18}$$

and

$$\nabla_t^2\Psi[\frac{\gamma\mu_2\epsilon_f}{k_o\Delta}+\frac{j\alpha}{k_o\epsilon_f}(\frac{\gamma^2}{\Delta}(\mu_1\epsilon_f-\gamma^2)-1)]-jk_o\alpha\Psi=0 \tag{3.19}$$

For a non-trivial solution, the determinant of these two equations must be equal to zero, which results in a second order equation in α, given below.

$$\alpha^2+j[(\mu_1\epsilon_f-\gamma^2)(\frac{-1}{\gamma\mu_2}+\frac{\gamma}{\mu_2\epsilon_f}) -\frac{\Delta}{\gamma\mu_2\epsilon_f}]\alpha+\epsilon_f=0 \tag{3.20}$$

Thus the proportionality constant can be determined from above and it has two solutions. Equations (3.18) and (3.19) can be re-arranged and written in the form shown below:

$$\nabla_t^2\Psi_1+u_1^2\Psi_1=0 \tag{3.21}$$

and

$$\nabla_t^2\Psi_2+u_2^2\Psi_2=0 \tag{3.22}$$

where

$$u_{1,2}^2=\frac{jk_o^2\Delta}{-j(\mu_1\epsilon_f-\gamma^2)+\gamma\mu_2\alpha_{1,2}} \tag{3.23}$$

Equations (3.21) and (3.22) are nothing but Bessel equations for which the solutions are

$$\Psi_1 = A_1 J_n(u_1 r) + B_1 N_n(u_1 r) \tag{3.24}$$

and

$$\Psi_2 = A_2 J_n(u_2 r) + B_2 N_n(u_2 r) \tag{3.25}$$

Hence the general solutions for E_z and H_z are given as follows:

$$E_z = \Psi_1 + \Psi_2 \tag{3.26}$$

Therefore,

$$E_z = A_1 J_n(u_1 r) + B_1 N_n(u_1 r) + A_2 J_n(u_2 r) + B_2 N_n(u_2 r) \tag{3.27}$$

and

$$H_z = \alpha_1 \Psi_1 + \alpha_2 \Psi_2 \tag{3.28}$$

Therefore,

$$H_z = A_1 y(u_1) J_n(u_1 r) + B_1 y(u_1) N_n(u_1 r) + A_2 y(u_2) J_n(u_2 r) + B_2 y(u_2) N_n(u_2 r) \tag{3.29}$$

where $y(u_1)$ and $y(u_2)$ represent α_1 and α_2. Thus the expressions for the longitudinal electric and magnetic field components are obtained. In the above equations the constants A_1, A_2, B_1 and B_2 are determined by applying appropriate boundary conditions. As can be seen the waves occuring in this waveguide are of the hybrid type in which the modes are mixed i.e. neither they are purely transverse electric (TE) nor transverse magnetic (TM) modes.

In the dielectric region the permeability is a constant and by adopting the same procedure used for the ferrite region, the field solutions in the dielectric region where the medium is homogeneous are given as follows:

$$E_r = \frac{1}{k_o(\epsilon_d - \gamma^2)}[j\gamma \frac{dE_z}{dr} - \frac{n}{r} H_z] \tag{3.30}$$

$$E_\phi = -\frac{1}{k_o(\epsilon_d - \gamma^2)}[\gamma\frac{n}{r}E_z + j\frac{dH_z}{dr}] \tag{3.31}$$

$$H_r = \frac{1}{k_o(\epsilon_d - \gamma^2)}[\epsilon_d\frac{n}{r}E_z + j\gamma\frac{dH_z}{dr}] \tag{3.32}$$

$$H_\phi = \frac{1}{k_o(\epsilon_d - \gamma^2)}[j\epsilon_d\frac{dE_z}{dr} - \gamma\frac{n}{r}H_z] \tag{3.33}$$

$$E_z = CJ_n(hr) + DN_n(hr) \tag{3.34}$$

$$H_z = EJ_n(hr) + FN_n(hr) \tag{3.35}$$

where $h^2 = k_o^2(\epsilon_d - \gamma^2)$. The constants C, D, E and F are determined by using the boundary conditions.

Now the necessary boundary conditions are applied to the different regions. Considering region:1 (dielectric where $a \leq r \leq b$), applying the conditions $E_z(r = a) = 0$ and $\frac{dH_z}{dr}|_{(r=a)} = 0$ leads to $D = -C\frac{J_n(h_1a)}{N_n(h_1a)}$ and $F = -E\frac{J_n'(h_1a)}{N_n'(h_1a)}$ respectively. By simple substitutions the following expressions are obtained.

$$E_{z1} = C_1[N_n(h_1a)J_n(h_1r) - J_n(h_1a)N_n(h_1r)] \tag{3.36}$$

where $C_1 = C/N_n(h_1a)$ and

$$H_{z1} = D_1[N_n'(h_1a)J_n(h_1r) - J_n'(h_1a)N_n(h_1r)] \tag{3.37}$$

where $D_1 = E/N_n'(h_1a)$ and $h_1^2 = k_o^2(\epsilon_1 - \gamma^2)$. Applying the same conditions to region 3 (dielectric (ϵ_3) where $c \leq r \leq d$) except that here $r = d$ in place of $r = a$, leads to the expressions given below

$$E_{z3} = C_3[N_n(h_3d)J_n(h_3r) - J_n(h_3d)N_n(h_3r)] \tag{3.38}$$

where $C_3 = C/N_n(h_3d)$ and

$$H_{z3} = D_3[N_n'(h_3d)J_n(h_3r) - J_n'(h_3d)N_n(h_3r)] \tag{3.39}$$

where $D_3 = E/N_n'(h_3d)$ and $h_3^2 = k_o^2(\epsilon_3 - \gamma^2)$. Next the boundary conditions are applied to region 2 (ferrite where $b \leq r \leq c$) as follows:

First of all, by applying the continuity of H_z at both the ferrite-dielectric interface namely at $r = b$ and at $r = c$ expressions are obtained for D_1 and D_3.

$$D_1 = \frac{[A_1 y(u_1) J_n(u_1 b) + B_1 y(u_1) N_n(u_1 b) + A_2 y(u_2) J_n(u_2 b) + B_2 y(u_2) N_n(u_2 b)]}{[N_n'(h_1 a) J_n(h_1 b) - J_n'(h_1 a) N_n(h_1 b)]} \tag{3.40}$$

and

$$D_3 = \frac{[A_1 y(u_1) J_n(u_1 c) + B_1 y(u_1) N_n(u_1 c) + A_2 y(u_2) J_n(u_2 c) + B_2 y(u_2) N_n(u_2 c)]}{[N_n'(h_3 d) J_n(h_3 c) - J_n'(h_3 d) N_n(h_3 c)]} \tag{3.41}$$

Similarly applying the continuity of E_z we have,

$$C_1 = \frac{[A_1 J_n(u_1 b) + B_1 N_n(u_1 b) + A_2 J_n(u_2 b) + B_2 N_n(u_2 b)]}{[N_n(h_1 a) J_n(h_1 b) - J_n(h_1 a) N_n(h_1 b)]} \tag{3.42}$$

and

$$C_3 = \frac{[A_1 J_n(u_1 c) + B_1 N_n(u_1 c) + A_2 J_n(u_2 c) + B_2 N_n(u_2 c)]}{[N_n(h_3 d) J_n(h_3 c) - J_n(h_3 d) N_n(h_3 c)]} \tag{3.43}$$

Now we apply the boundary condition that the normal component of the induction field (B_N) is continuous at the ferrite-dielectric interface ($r = b$).

$$B_{N2}(ferrite) = B_{N1}(dielectric)$$

Therefore

$$[\mu_1 H_{r2} + j\mu_2 H_{\phi 2}]_{r=b-} = H_{r1}|_{r=b+}$$

Making the relevant substitutions the right hand side (RHS)of the above equation is found to be

$$\begin{aligned} RHS \;=\; & \frac{1}{k_o(\epsilon_1 - \gamma^2)}[A_1 J_n(u_1 b)(\epsilon_1 \frac{n}{b} + j\gamma H_n(h_1, a, b) y(u_1)) \\ & + A_2 J_n(u_2 b)(\epsilon_1 \frac{n}{b} + j\gamma H_n(h_1, a, b) y(u_2)) \\ & + B_1 N_n(u_1 b)(\epsilon_1 \frac{n}{b} + j\gamma H_n(h_1, a, b) y(u_1)) \\ & + B_2 N_n(u_2 b)(\epsilon_1 \frac{n}{b} + j\gamma H_n(h_1, a, b) y(u_2))] \end{aligned} \tag{3.44}$$

where

$$H_n(h_1,a,b)=\frac{N_n'(h_1a)J_n'(h_1b)-J_n'(h_1a)N_n'(h_1b)}{N_n'(h_1a)J_n(h_1b)-J_n'(h_1a)N_n(h_1b)} \tag{3.45}$$

and the left hand side (LHS) is found to be

$$\begin{aligned}
LHS \;=\; & \frac{1}{k_o\Delta}[A_1J_n(u_1b)(-(B\mu_1-A\mu_2)[\epsilon_f\frac{J_n'(u_1b)}{J_n(u_1b)}+j\gamma\frac{n}{b}y(u_1)] \\
& +(B\mu_2-A\mu_1)[\epsilon_f\frac{n}{b}+j\gamma y(u_1)\frac{J_n'(u_1b)}{J_n(u_1b)}]) \\
& +A_2J_n(u_2b)(-(B\mu_1-A\mu_2)[\epsilon_f\frac{J_n'(u_2b)}{J_n(u_2b)}+j\gamma\frac{n}{b}y(u_2)] \\
& +(B\mu_2-A\mu_1)[\epsilon_f\frac{n}{b}+j\gamma y(u_2)\frac{J_n'(u_2b)}{J_n(u_2b)}]) \\
& +B_1N_n(u_1b)(-(B\mu_1-A\mu_2)[\epsilon_f\frac{N_n'(u_1b)}{N_n(u_1b)}+j\gamma\frac{n}{b}y(u_1)] \\
& +(B\mu_2-A\mu_1)[\epsilon_f\frac{n}{b}+j\gamma y(u_1)\frac{N_n'(u_1b)}{N_n(u_1b)}]) \\
& +B_2N_n(u_2b)(-(B\mu_1-A\mu_2)[\epsilon_f\frac{N_n'(u_2b)}{N_n(u_2b)}+j\gamma\frac{n}{b}y(u_2)] \\
& +(B\mu_2-A\mu_1)[\epsilon_f\frac{n}{b}+j\gamma y(u_2)\frac{N_n'(u_2b)}{N_n(u_2b)}])]
\end{aligned} \tag{3.46}$$

where $A=(\mu_1\epsilon_f-\gamma^2)$ and $B=\mu_2\epsilon_f$. From equations (3.44) and (3.46) after simplification we get

$$\begin{aligned}
& A_1J_n(u_1b)f(u_1,h_1)+A_2J_n(u_2b)f(u_2,h_1) \\
& +B_1N_n(u_1b)g(u_1,h_1)+B_2N_n(u_2b)g(u_2,h_1)=0
\end{aligned} \tag{3.47}$$

where

$$\begin{aligned}
f(u_i,h_1) \;=\; & \frac{1}{\Delta}[-(B\mu_1-A\mu_2)(\epsilon_f\frac{J_n'(u_ib)}{J_n(u_ib)}+j\gamma\frac{n}{b}y(u_i)) \\
& +(B\mu_2-A\mu_1)(\epsilon_f\frac{n}{b}+j\gamma y(u_i)\frac{J_n'(u_ib)}{J_n(u_ib)})] \\
& -\frac{1}{\epsilon_1-\gamma^2}[\epsilon_1\frac{n}{b}+j\gamma H_n(h_1,a,b)y(u_i)]
\end{aligned} \tag{3.48}$$

$$g(u_i,h_1) \;=\; \frac{1}{\Delta}[-(B\mu_1-A\mu_2)(\epsilon_f\frac{N_n'(u_ib)}{N_n(u_ib)}+j\gamma\frac{n}{b}y(u_i))$$

$$+(B\mu_2 - A\mu_1)(\epsilon_f \frac{n}{b} + j\gamma y(u_i)\frac{N_n'(u_i b)}{N_n(u_i b)})]$$
$$-\frac{1}{\epsilon_1 - \gamma^2}[\epsilon_1 \frac{n}{b} + j\gamma H_n(h_1, a, b)y(u_i)] \quad (3.49)$$

and $i = 1, 2$. Now using the boundary condition $H_{\phi 1}(dielectric) = H_{\phi 2}(ferrite)$ at $r = b$, we can obtain another relation involving A_1, A_2, B_1 and B_2 as follows: First an expression for the LHS of the boundary condition stated above is obtained after making the required substitutions as

$$\begin{aligned} LHS \;=\; & \frac{1}{k_o(\epsilon_1 - \gamma^2)}[A_1 J_n(u_1 b)[j\epsilon_1 G_n(h_1, a, b) - \gamma \frac{n}{b} y(u_1)] \\ & + A_2 J_n(u_2 b)[j\epsilon_1 G_n(h_1, a, b) - \gamma \frac{n}{b} y(u_2)] \\ & + B_1 N_n(u_1 b)[j\epsilon_1 G_n(h_1, a, b) - \gamma \frac{n}{b} y(u_1)] \\ & + B_2 N_n(u_2 b)[j\epsilon_1 G_n(h_1, a, b) - \gamma \frac{n}{b} y(u_2)]] \end{aligned} \quad (3.50)$$

where

$$G_n(h_1, a, b) = \frac{N_n(h_1 a)J_n'(h_1 b) - J_n(h_1 a)N_n'(h_1 b)}{N_n(h_1 a)J_n(h_1 b) - J_n(h_1 a)N_n(h_1 b)} \quad (3.51)$$

and RHS is obtained as given below:

$$\begin{aligned} RHS \;=\; & \frac{1}{k_o \Delta}[A_1 J_n(u_1 b)(-j\epsilon_f A\frac{J_n'(u_1 b)}{J_n(u_1 b)} + B\gamma y(u_1)\frac{J_n'(u_1 b)}{J_n(u_1 b)} - j\epsilon_f B\frac{n}{b} + A\gamma \frac{n}{b} y(u_1)) \\ & + A_2 J_n(u_2 b)(-j\epsilon_f A\frac{J_n'(u_2 b)}{J_n(u_2 b)} + B\gamma y(u_2)\frac{J_n'(u_2 b)}{J_n(u_2 b)} - j\epsilon_f B\frac{n}{b} + A\gamma \frac{n}{b} y(u_2)) \\ & + B_1 N_n(u_1 b)(-j\epsilon_f A\frac{N_n'(u_1 b)}{N_n(u_1 b)} + B\gamma y(u_1)\frac{N_n'(u_1 b)}{N_n(u_1 b)} - j\epsilon_f B\frac{n}{b} + A\gamma \frac{n}{b} y(u_1)) \\ & + B_2 N_n(u_2 b)(-j\epsilon_f A\frac{N_n'(u_2 b)}{N_n(u_2 b)} + B\gamma y(u_2)\frac{N_n'(u_2 b)}{N_n(u_2 b)} - j\epsilon_f B\frac{n}{b} + A\gamma \frac{n}{b} y(u_2))] \end{aligned} \quad (3.52)$$

Equating (3.50) and (3.52) we get

$$\begin{aligned} & A_1 J_n(u_1 b)p(u_1, h_1) + A_2 J_n(u_2 b)p(u_2, h_1) \\ & + B_1 N_n(u_1 b)q(u_1, h_1) + B_2 N_n(u_2 b)q(u_2, h_1) = 0 \end{aligned} \quad (3.53)$$

where

$$p(u_i,h_1) = \frac{1}{\Delta}[-(j\epsilon_f A - B\gamma y(u_i))\frac{J_n'(u_i b)}{J_n(u_i b)} + \frac{n}{b}(A\gamma y(u_i) - jB\epsilon_f)]$$
$$- \frac{1}{\epsilon_1 - \gamma^2}[(j\epsilon_1 G_n(h_1,a,b) - \frac{n}{b}\gamma y(u_i)] \quad (3.54)$$

$$q(u_i,h_1) = \frac{1}{\Delta}[-(j\epsilon_f A - B\gamma y(u_i))\frac{N_n'(u_i b)}{N_n(u_i b)} + \frac{n}{b}(A\gamma y(u_i) - jB\epsilon_f)]$$
$$- \frac{1}{\epsilon_1 - \gamma^2}[(j\epsilon_1 G_n(h_1,a,b) - \frac{n}{b}\gamma y(u_i)] \quad (3.55)$$

and $i = 1,2$. Now applying the same boundary conditions to the other ferrite-dielectric interface ($r = c$) we arrive at the following relations listed below:

$$A_1 J_n(u_1 c) f(u_1,h_3) + A_2 J_n(u_2 c) f(u_2,h_3)$$
$$+B_1 N_n(u_1 c) g(u_1,h_3) + B_2 N_n(u_2 c) g(u_2,h_3) = 0 \quad (3.56)$$

where

$$f(u_i,h_3) = \frac{1}{\Delta}[-(B\mu_1 - A\mu_2)(\epsilon_f \frac{J_n'(u_i c)}{J_n(u_i c)} + j\gamma\frac{n}{c}y(u_i))$$
$$+ (B\mu_2 - A\mu_1)(\epsilon_f\frac{n}{c} + j\gamma y(u_i)\frac{J_n'(u_i c)}{J_n(u_i c)})]$$
$$- \frac{1}{\epsilon_3 - \gamma^2}[\epsilon_3\frac{n}{c} + j\gamma H_n(h_3,c,d)y(u_i)] \quad (3.57)$$

$$g(u_i,h_3) = \frac{1}{\Delta}[-(B\mu_1 - A\mu_2)(\epsilon_f \frac{N_n'(u_i c)}{N_n(u_i c)} + j\gamma\frac{n}{c}y(u_i))$$
$$+ (B\mu_2 - A\mu_1)(\epsilon_f\frac{n}{c} + j\gamma y(u_i)\frac{N_n'(u_i c)}{N_n(u_i c)})]$$
$$- \frac{1}{\epsilon_3 - \gamma^2}[\epsilon_3\frac{n}{c} + j\gamma H_n(h_3,c,d)y(u_i)] \quad (3.58)$$

$$H_n(h_3,c,d) = \frac{N_n'(h_3 d)J_n'(h_3 c) - J_n'(h_3 d)N_n'(h_3 c)}{N_n'(h_3 d)J_n(h_3 c) - J_n'(h_3 d)N_n(h_3 c)} \quad (3.59)$$

and

$$A_1 J_n(u_1 c) p(u_1,h_3) + A_2 J_n(u_2 c) p(u_2,h_3)$$
$$+B_1 N_n(u_1 c) q(u_1,h_3) + B_2 N_n(u_2 c) q(u_2,h_3) = 0 \quad (3.60)$$

where

$$p(u_i,h_3) = \frac{1}{\Delta}[-(j\epsilon_f A - B\gamma y(u_i))\frac{J_n'(u_i c)}{J_n(u_i c)} + \frac{n}{c}(A\gamma y(u_i) - jB\epsilon_f)] - \frac{1}{\epsilon_3 - \gamma^2}[(j\epsilon_3 G_n(h_3,c,d) - \frac{n}{c}\gamma y(u_i)] \quad (3.61)$$

$$q(u_i,h_3) = \frac{1}{\Delta}[-(j\epsilon_f A - B\gamma y(u_i))\frac{N_n'(u_i c)}{N_n(u_i c)} + \frac{n}{c}(A\gamma y(u_i) - jB\epsilon_f)] - \frac{1}{\epsilon_3 - \gamma^2}[(j\epsilon_3 G_n(h_3,c,d) - \frac{n}{c}\gamma y(u_i)] \quad (3.62)$$

$$G_n(h_3,c,d) = \frac{N_n(h_3 d)J_n'(h_3 c) - J_n(h_3 d)N_n'(h_3 c)}{N_n(h_3 d)J_n(h_3 c) - J_n(h_3 d)N_n(h_3 c)} \quad (3.63)$$

and $i = 1,2$. Now that we have four equations and four unknowns, we can solve for the dispersion relations by first determining the constants B_1 and B_2 from equations (3.47) and (3.53) and then substituting for the same in equations (3.56) and (3.60). The two dispersion equations are obtained and dividing one by the other eliminates A_1 and A_2 to yield the required expression which is given as follows:

$$\frac{F_\phi(u_1)}{F_r(u_1)} = \frac{F_\phi(u_2)}{F_r(u_2)} \quad (3.64)$$

$$F_\phi(u_i) = [J_n(u_i c)f(u_i,h_3) + \frac{J_n(u_i b)}{N_n(u_1 b)}(\frac{p(u_i,h_1)g(u_2,h_1) - f(u_i,h_1)q(u_2,h_1)}{g(u_1,h_1)q(u_2,h_1) - g(u_2,h_1)q(u_1,h_1)}) N_n(u_1 c)g(u_1,h_3) + \frac{J_n(u_i b)}{N_n(u_2 b)}(\frac{f(u_i,h_1)q(u_1,h_1) - p(u_i,h_1)g(u_1,h_1)}{g(u_1,h_1)q(u_2,h_1) - g(u_2,h_1)q(u_1,h_1)}) N_n(u_2 c)g(u_2,h_3)] \quad (3.65)$$

$$F_r(u_i) = [J_n(u_i c)p(u_i,h_3) + \frac{J_n(u_i b)}{N_n(u_1 b)}(\frac{p(u_i,h_1)g(u_2,h_1) - f(u_i,h_1)q(u_2,h_1)}{g(u_1,h_1)q(u_2,h_1) - g(u_2,h_1)q(u_1,h_1)}) N_n(u_1 c)q(u_1,h_3) + \frac{J_n(u_i b)}{N_n(u_2 b)}(\frac{f(u_i,h_1)q(u_1,h_1) - p(u_i,h_1)g(u_1,h_1)}{g(u_1,h_1)q(u_2,h_1) - g(u_2,h_1)q(u_1,h_1)}) N_n(u_2 c)q(u_2,h_3)] \quad (3.66)$$

where $i = 1,2$ and $u_{1,2}^2$ is expanded to

$$u_{1,2}^2 = k_o^2[\frac{\epsilon_f(1+2\Omega_H) + (\epsilon_f - \gamma^2)(2\Omega_H^2 + \Omega_H - 2\Omega^2)}{2(\Omega_H^2 + \Omega_H - \Omega^2)}]$$

$$\pm \frac{[(\Omega_H^2\gamma^2 - \epsilon_f(\Omega_H^2 + \Omega_H - 2\Omega^2))^2 + 4\epsilon_f^2\Omega^2(\Omega_H^2 + \Omega_H - \Omega^2)]^{1/2}}{2\Omega_H(\Omega_H^2 + \Omega_H - \Omega^2)} \quad (3.67)$$

Equations (3.64) through (3.67) generally form the exact dispersion relations. For a completely filled waveguide, $b = a$ and $c = d$ are employed in these expressions. Before solving the general dispersion relations it is very important to derive the dispersion relation at cutoff and then solve them by numerical techniques for obtaining the desired dispersion characteristics.

3.2 Dispersion relations at cutoff

Cutoff frequency is defined as the frequency at which propagation begins namely at $\gamma = 0$. The dispersion relations are now derived by setting $\gamma = 0$. The equations (3.9), (3.10), (3.14) and (3.15) become:

$$E_r = -\frac{n}{k_o\epsilon_f}\frac{1}{r}H_z \quad (3.68)$$

$$E_\phi = -\frac{j}{k_o\epsilon_f}\frac{dH_z}{dr} \quad (3.69)$$

$$H_r = -\frac{1}{Det}[\frac{\mu_1}{k_o}\frac{n}{r}E_z + \frac{\mu_2}{k_o}\frac{dE_z}{dr}] \quad (3.70)$$

$$H_\phi = -\frac{j}{Det}[\frac{\mu_1}{k_o}\frac{dE_z}{dr} + \frac{\mu_2}{k_o}\frac{n}{r}E_z] \quad (3.71)$$

where $Det = [\mu_2^2 - \mu_1^2]$. Now by substituting E_r in (3.68) and E_ϕ in (3.69) into the longitudinal component of the Maxwell's equation (3.8), the wave equation for only H_z is obtained:

$$\nabla_t^2 H_z + k_o^2\eta_2^2 H_z = 0 \quad (3.72)$$

where $\eta_2^2 = \epsilon_f$

Similarly by substituting H_r in (3.70) and H_ϕ in (3.71) into the longitudinal component of the Maxwell's equation (3.5), the wave equation for only E_z is obtained:

$$\nabla_t^2 E_z + k_o^2\eta_1^2 E_z = 0 \quad (3.73)$$

where $\eta_1^2 = \frac{[\mu_1^2 - \mu_2^2]}{\mu_1}\epsilon_f$

Therefore it is obvious that waves at the cutoff frequency are no more hybrid but split up into purely transverse electric (TE) modes and transverse magnetic (TM) modes.

3.2.1 Dispersion relations for TE modes

The longitudinal component in the ferrite region is written as:

$$H_{z2} = A_2 J_n(k_o \eta_2 r) + B_2 N_n(k_o \eta_2 r) \tag{3.74}$$

The field solutions in the dielectric region are given as follows:

$$E_r = -\frac{1}{k_o \epsilon_1}\frac{n}{r} H_z \tag{3.75}$$

$$E_\phi = -\frac{j}{k_o \epsilon_1}\frac{dH_z}{dr} \tag{3.76}$$

and

$$H_z = E J_n(h_1 r) + F N_n(h_1 r) \tag{3.77}$$

where $h_1^2 = k_o^2 \epsilon_1$.

As before in region 1 we have

$$H_{z1} = D_1[N_n'(h_1 a) J_n(h_1 r) - J_n'(h_1 a) N_n(h_1 r)] \tag{3.78}$$

and in region 3

$$H_{z3} = D_3[N_n'(h_3 d) J_n(h_3 r) - J_n'(h_3 d) N_n(h_3 r)] \tag{3.79}$$

where $h_3^2 = k_o^2 \epsilon_3$.

The boundary conditions are now applied in region 2 to obtain the dispersion relations. First by applying the condition $E_{\phi 1}(r = b)$ dielectric $= E_{\phi 2}(r = b)$ ferrite we get

$$A_2[H_n(h_1, a, b) - \frac{\epsilon_1}{\epsilon_f}\frac{J_n'(k_o \eta_2 b)}{J_n(k_o \eta_2 b)}] J_n(k_o \eta_2 b)$$
$$= -B_2[H_n(h_1, a, b) - \frac{\epsilon_1}{\epsilon_f}\frac{N_n'(k_o \eta_2 b)}{N_n(k_o \eta_2 b)}] N_n(k_o \eta_2 b) \tag{3.80}$$

Applying the same condition except that $r = c$ instead of $r = b$ we have

$$A_2[H_n(h_3, c, d) - \frac{\epsilon_3}{\epsilon_f}\frac{J_n'(k_o\eta_2 c)}{J_n(k_o\eta_2 c)}]J_n(k_o\eta_2 c)$$
$$= -B_2[H_n(h_3, c, d) - \frac{\epsilon_3}{\epsilon_f}\frac{N_n'(k_o\eta_2 c)}{N_n(k_o\eta_2 c)}]N_n(k_o\eta_2 c) \tag{3.81}$$

Dividing one equation by the other eliminates the constants A_2 and B_2 resulting in

$$\frac{[H_n(h_3, c, d) - \frac{\epsilon_3}{\epsilon_f}\frac{J_n'(k_o\eta_2 c)}{J_n(k_o\eta_2 c)}]J_n(k_o\eta_2 c)}{[H_n(h_1, a, b) - \frac{\epsilon_3}{\epsilon_f}\frac{J_n'(k_o\eta_2 b)}{J_n(k_o\eta_2 b)}]J_n(k_o\eta_2 b)}$$
$$= \frac{[H_n(h_3, c, d) - \frac{\epsilon_3}{\epsilon_f}\frac{N_n'(k_o\eta_2 c)}{N_n(k_o\eta_2 c)}]N_n(k_o\eta_2 c)}{[H_n(h_1, a, b) - \frac{\epsilon_3}{\epsilon_f}\frac{N_n'(k_o\eta_2 b)}{N_n(k_o\eta_2 b)}]N_n(k_o\eta_2 b)} \tag{3.82}$$

The above equation along with $\eta_2^2 = \epsilon_f$ form the dispersion relation at cutoff for the TE modes.

As can be seen, the dispersion equations for the TE modes are independent of both the gyromagnetic frequency (Ω_H) and the sign of the azimuthal variation number (n). The reason for the Ω_H independence is that at cutoff the RF magnetic field is longitudinal to the dc magnetic field H_o, therefore the ac magnetic field has no effect on the motion of the magnetization vector and hence unaffected by H_o.

3.2.2 Dispersion relations for TM modes

The longitudinal component in the ferrite region is written as:

$$E_{z2} = A_1 J_n(k_o\eta_1 r) + B_1 N_n(k_o\eta_1 r) \tag{3.83}$$

The field solutions in the dielectric region are given as follows:

$$H_r = \frac{1}{k_o}\frac{n}{r}E_z \tag{3.84}$$

$$H_\phi = \frac{j}{k_o}\frac{dE_z}{dr} \tag{3.85}$$

and

$$E_z = CJ_n(h_1 r) + DN_n(h_1 r) \tag{3.86}$$

As before in region 1 we have

$$E_{z1} = C_1[N_n(h_1 a)J_n(h_1 r) - J_n(h_1 a)N_n(h_1 r)] \tag{3.87}$$

and in region 3

$$E_{z3} = C_3[N_n(h_3 d)J_n(h_3 r) - J_n(h_3 d)N_n(h_3 r)] \tag{3.88}$$

Next by using the boundary condition B_{N1} (dielectric) = B_{N2} (ferrite) both at $r = b$ and $r = c$ results in two other relations namely

$$\begin{aligned} &C_1[N_n(h_1 a)J_n(h_1 b) - J_n(h_1 a)N_n(h_1 b)] \\ &\quad = A_1 J_n(k_o \eta_1 b) + B_1 N_n(k_o \eta_1 b) \end{aligned} \tag{3.89}$$

and

$$\begin{aligned} &C_3[N_n(h_3 d)J_n(h_3 c) - J_n(h_3 d)N_n(h_3 c)] \\ &\quad = A_1 J_n(k_o \eta_1 c) + B_1 N_n(k_o \eta_1 c) \end{aligned} \tag{3.90}$$

Now finally applying the boundary condition $H_{\phi 1}$ (dielectric) = $H_{\phi 2}$ (ferrite) both at $r = b$ and $r = c$ and then making use of equations (3.89) and (3.90) we arrive at the following relations

$$\begin{aligned} &A_1[-\frac{\mu_2 \epsilon_f^2}{Det}\frac{n}{b} - \frac{\mu_1 \epsilon_f^2}{Det}\frac{J_n'(k_o \eta_1 b)}{J_n(k_o \eta_1 b)} - G_n(h_1, a, b)]J_n(k_o \eta_1 b) \\ &= -B_1[-\frac{\mu_2 \epsilon_f^2}{Det}\frac{n}{b} - \frac{\mu_1 \epsilon_f^2}{Det}\frac{N_n'(k_o \eta_1 b)}{N_n(k_o \eta_1 b)} - G_n(h_1, a, b)]N_n(k_o \eta_1 b) \end{aligned} \tag{3.91}$$

and

$$\begin{aligned} &A_1[-\frac{\mu_2 \epsilon_f^2}{Det}\frac{n}{c} - \frac{\mu_1 \epsilon_f^2}{Det}\frac{J_n'(k_o \eta_1 c)}{J_n(k_o \eta_1 c)} - G_n(h_3, c, d)]J_n(k_o \eta_1 c) \\ &= -B_1[-\frac{\mu_2 \epsilon_f^2}{Det}\frac{n}{c} - \frac{\mu_1 \epsilon_f^2}{Det}\frac{N_n'(k_o \eta_1 c)}{N_n(k_o \eta_1 c)} - G_n(h_1, c, d)]N_n(k_o \eta_1 c) \end{aligned} \tag{3.92}$$

Dividing one equation by the other eliminates the constants A_1 and B_1 resulting in

$$\frac{J_n(k_o\eta_1 c)[-\frac{\mu_2\epsilon_f^2}{Det}\frac{n}{c} - \frac{\mu_1\epsilon_f^2}{Det}\frac{J_n'(k_o\eta_1 c)}{J_n(k_o\eta_1 c)} - G_n(h_3,c,d)]}{J_n(k_o\eta_1 b)[-\frac{\mu_2\epsilon_f^2}{Det}\frac{n}{b} - \frac{\mu_1\epsilon_f^2}{Det}\frac{J_n'(k_o\eta_1 b)}{J_n(k_o\eta_1 b)} - G_n(h_1,a,b)]}$$
$$= \frac{N_n(k_o\eta_1 c)[-\frac{\mu_2\epsilon_f^2}{Det}\frac{n}{c} - \frac{\mu_1\epsilon_f^2}{Det}\frac{N_n'(k_o\eta_1 c)}{N_n(k_o\eta_1 c)} - G_n(h_1,c,d)]}{N_n(k_o\eta_1 b)[-\frac{\mu_2\epsilon_f^2}{Det}\frac{n}{b} - \frac{\mu_1\epsilon_f^2}{Det}\frac{N_n'(k_o\eta_1 b)}{N_n(k_o\eta_1 b)} - G_n(h_1,a,b)]} \tag{3.93}$$

The above equation along with $\eta_1^2 = \frac{[\mu_1^2-\mu_2^2]}{\mu_1}\epsilon_f$ constitute the dispersion relations for the TM modes at cutoff.

As can be, the dispersion relations for the TM modes depend on both the gyromagnetic frequency and the sign of the azimuthal variation number. The reason being, the RF magnetic field is in a direction perpendicular to the dc magnetic field, hence contributing to the motion of the magnetization vector and therefore affected by H_o.

3.3 Dispersion relations at resonance

As γ becomes very large almost tending to infinity the radial wave numbers are approximated as

$$\lim_{\gamma\to\infty}\eta_1^2 = -\frac{\gamma^2(\Omega_H^2-\Omega^2)}{\Omega_H^2+\Omega_H-\Omega^2} \tag{3.94}$$

and

$$\lim_{\gamma\to\infty}\eta_2^2 = -\gamma^2 \tag{3.95}$$

It has been found that there are no resonant frequencies in region I since the radial wave numbers are imaginary but in region II they are asymptotic to the gyromagnetic frequency Ω_H which in fact is the resonant frequency. Once the cutoff and resonant points are found, then intermediate points can be determined by a numerical method using the root search technique to complete the dispersion

curves for the dipolar modes. The numerical results for all the cases are discussed in the next chapter.

Chapter 4

NUMERICAL RESULTS

The dielectric constant of ferrite (ϵ_f) is equal to 12 and the dielectric constants for medium 1 and medium 3 are unity. The radius 'd' is assumed to be 4 times the radius 'a' as shown in Figure 1.1. For the partially filled ferrite case the spacing between 'b' and 'c' is equal to 'a' and $\frac{a}{b} = 0.5$ but for the almost fully filled ferrite case the spacing between 'b' and 'c' is widened thereby increasing the thickness of the ferrite ring in such a way that $\frac{c}{d} = \frac{a}{b} = 0.9$ and the normalized ferrite column radius q is taken as 0.5

The computational work is obtained based on each of the four parametric regions namely region I: where u_1 and u_2 are imaginary, region II: where u_1 is real and u_2 is imaginary, region III: where u_1 is imaginary and u_2 is real and region IV: where u_1 and u_2 are real.

4.1 Cutoffs and resonances

4.1.1 Dispersion characteristics for TE modes

Having obtained the dispersion relations for TE modes in the earlier chapter, in equation (3.82), it is important to solve them and plot the characteristics. The dispersion equation (3.82) is dependent on the radius ratio S_o and the normalized ferrite column radius q. Therefore the dispersion cueves are plotted Ω versus q

as indicated in Figure 4.1 for $S_o = 0.5$ and Figure 4.2 for $S_o = 0.9$. Each cutoff curve is designated as $TE_{n,p}^{S_o}$ where p denotes the increasing order of the cutoff frequency. As seen from the Figures 4.1 and 4.2 at constant S_o, the TE cutoff frequency decreases with an increase in q, but for a fixed value of q, the cutoff frequency decreases as S_o increases. As will be seen later, the TE cutoff dispersion curves determine the cutoff frequencies of various modes such as surface wave modes, volume modes and modified waveguide modes.

4.1.2 Dispersion characteristics for TM modes

The dispersion relations for TM modes at cutoff depends not only on S_o, q and the sign of n but also on Ω_H as seen in equation (3.93). The TM cutoff frequencies are plotted against Ω_H in Figure 4.3 for $S_o = 0.5$ and Figure 4.4 for $S_o = 0.9$. As can be seen the dotted curves $\Omega = \Omega_H + 1$ and $\Omega = \Omega_c$ (where $\Omega_c = [\Omega_H(\Omega_H + 1)]^{1/2}$) divide the $\Omega - \Omega_H$ plane into 3 distinct regions namely A,B and C. In the regions A and C, η_1 is real while in region B, η_1 is imaginary. The modes which fall in region A determine the cutoff frequency of the volume modes while those that fall in regions B and C determine the cutoff frequency of the surface and modified waveguide modes respectively. The cutoff curves $V_{n,p}^{S_o}$ start from Ω_c and increases rapidly along the curve $\Omega = \Omega_c$ with increases in Ω_H until they saturate when Ω_H becomes high. The cutoff curves $TM_{n,p}^{S_o}$ are asymptotic to the $\Omega = \Omega_H + 1$ or $\Omega = \Omega_c$ curves respectively.

4.2 Exact dispersion characteristics

The exact analysis predicts all possible modes, namely, the surface wave modes, the volume modes and the modified waveguide modes. The surface wave modes are designated as $S_n^{S_o}$ while the modified waveguide modes are designated as $TE_{n,m}^{S_o}$ or $TM_{n,m}^{S_o}$ depending upon whether their cutoff frequencies are determined by the TE

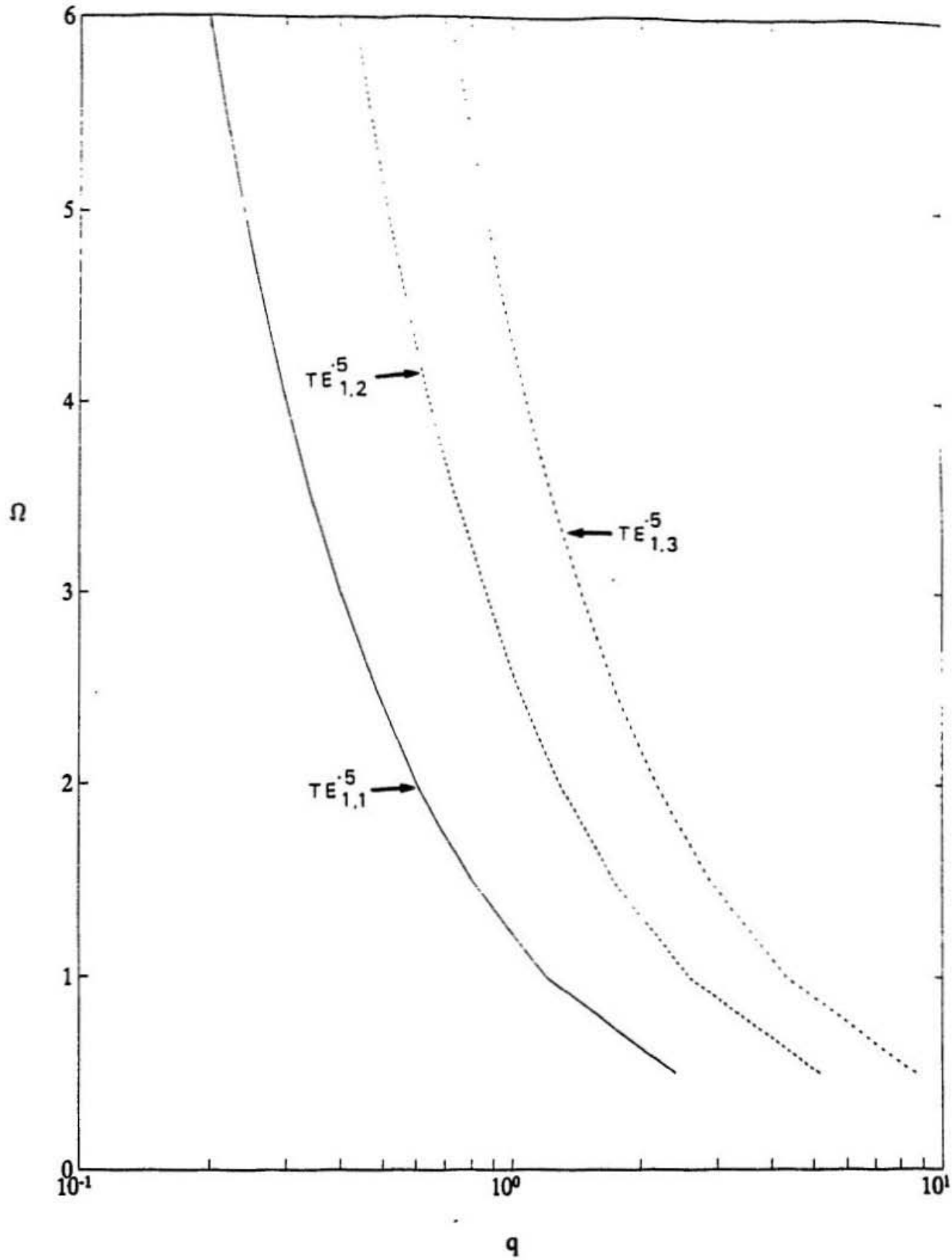

Figure 4.1: TE cutoff for $S_o = 0.5$, $n = \pm 1$

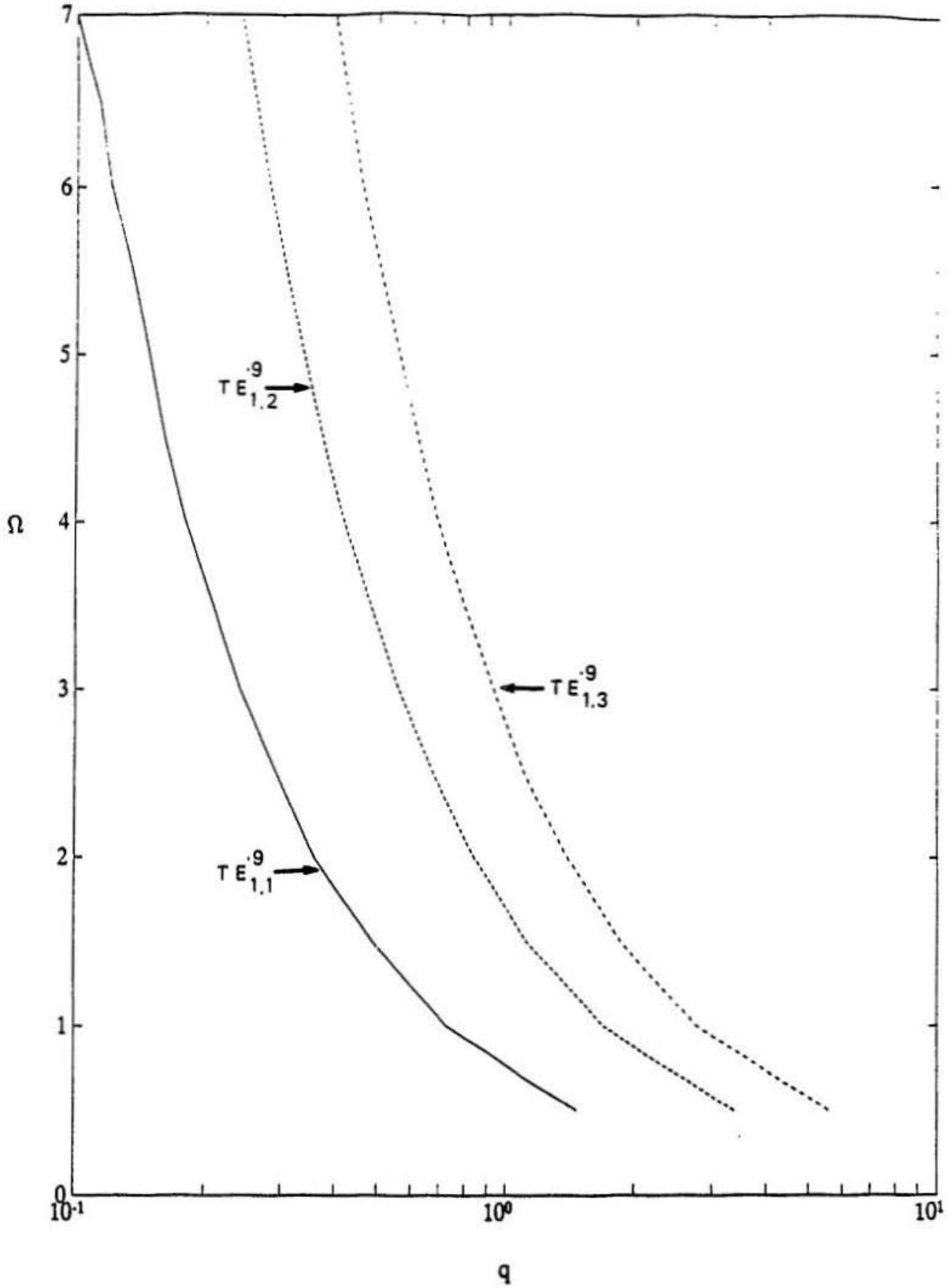

Figure 4.2: TE cutoff for $S_o = 0.9$, $n = \pm 1$

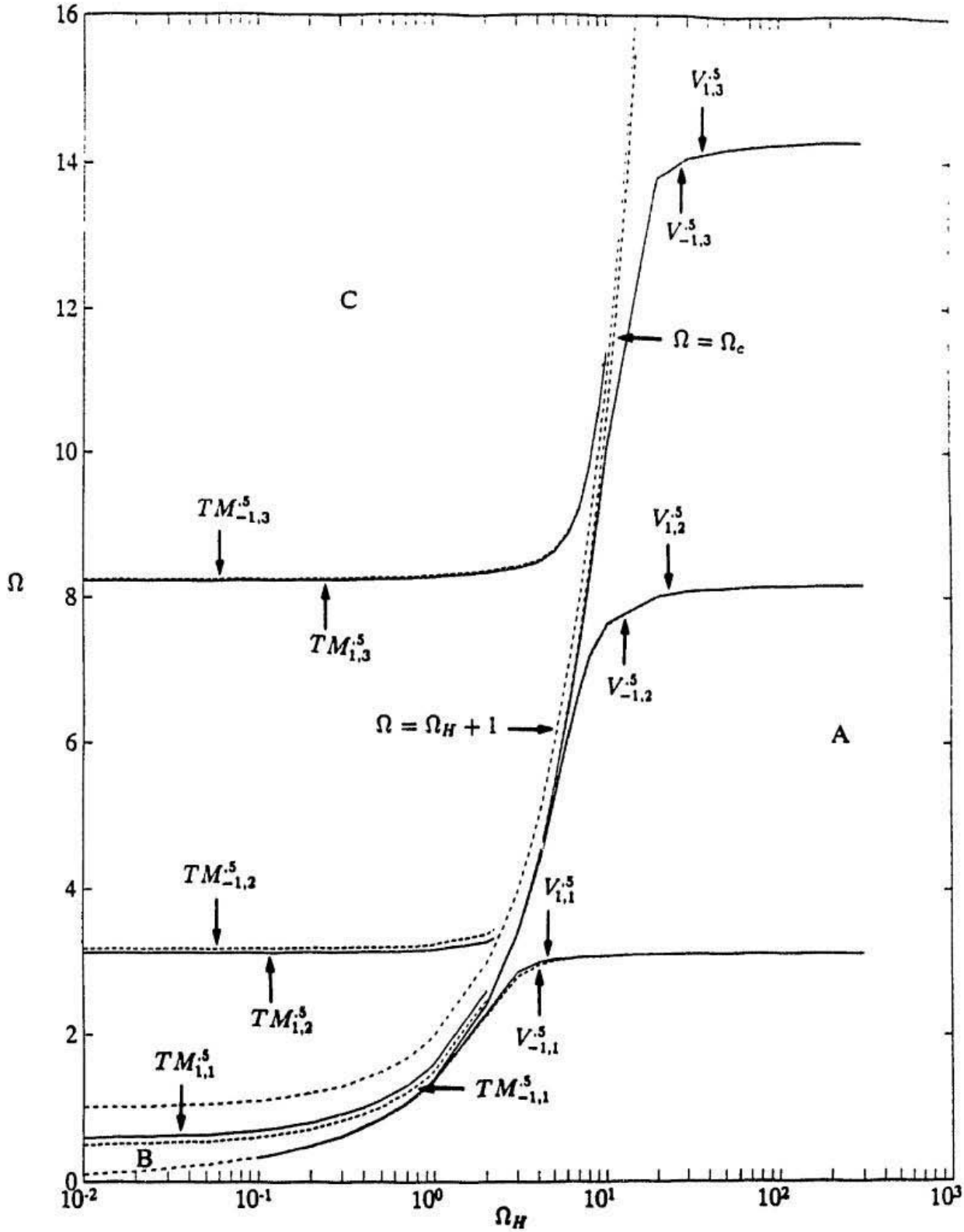

Figure 4.3: TM cutoff for $S_o = 0.5$, $n = \pm 1$

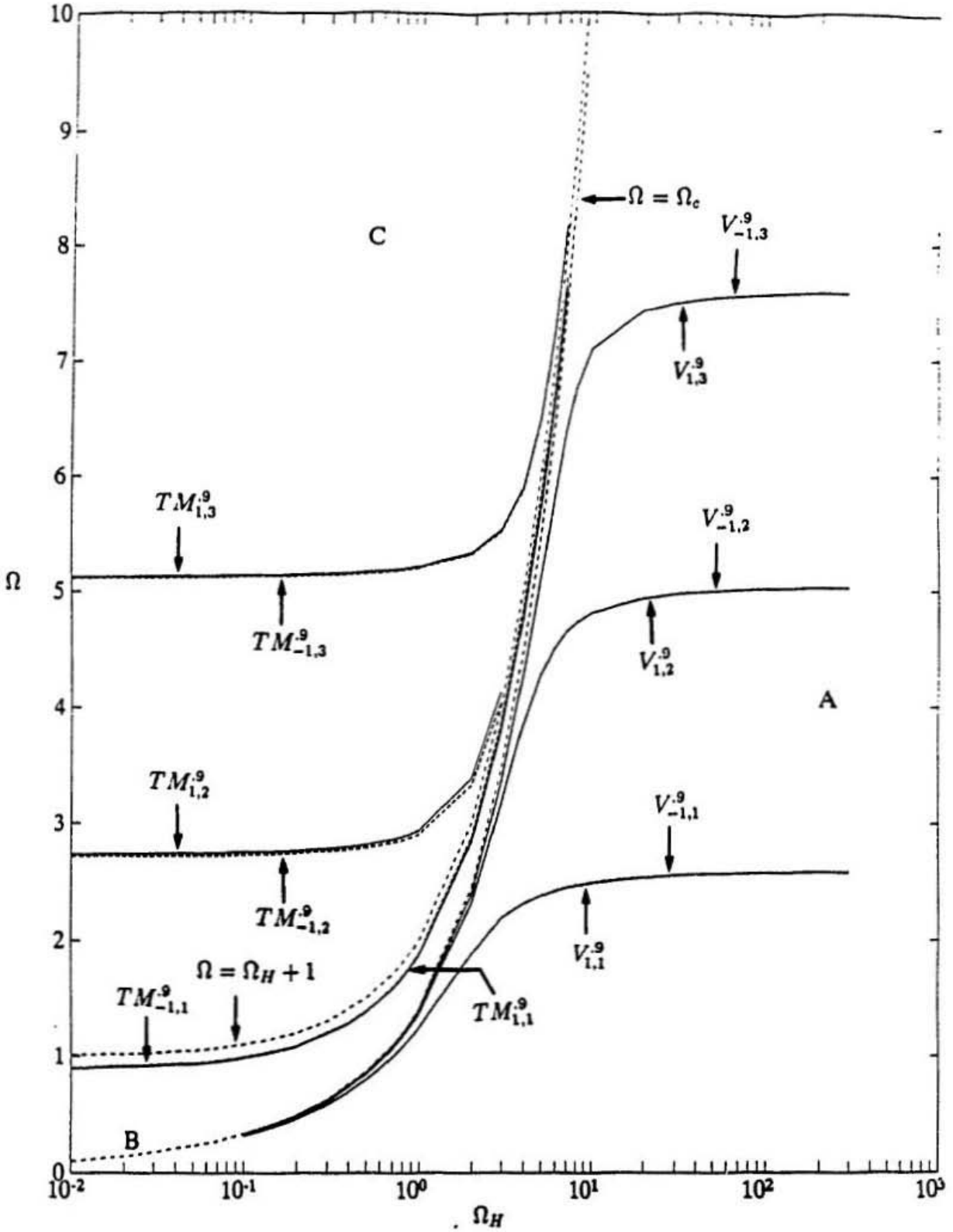

Figure 4.4: TM cutoff for $S_o = 0.9$, $n = \pm 1$

or TM cutoff curves. Since the TE cutoff frequencies take any values between zero and infinity, they determine the cutoff frequencies of all categories of modes. $TM_{n,p}^{S_o}$ cutoff curves determine the cutoff frequencies of both surface wave modes as well as modified waveguide modes. $V_{n,p}^{S_o}$ cutoff curves determine the cutoff frequencies of the volume modes.

The exact dispersion curves of the modes are shown in Figures 4.5 and 4.6 for a weak magnetic field ($\Omega_H < 1$) and in Figures 4.7 and 4.8 for a strong magnetic field ($\Omega_H > 1$). As can be seen for the cases where $\Omega_H = 0.5$, the surface wave modes exist. The surface wave modes terminate on the line $\Omega = \Omega_c$ thereby indicating the backward nature of these modes. Moreover the group velocity of these modes at the termination point is zero. An interesting result is observed, the surface wave modes exist even for $n = -1$ in both, the partially filled and the approximately fully filled cases of a coaxial waveguide unlike the circular waveguide case as illustrated in (Le-Ngoc, 1975). The cutoff point of the surface wave mode when $n = -1$ is different from that of the surface wave mode of $n = 1$ and also the surface wave mode curve when $n = -1$ terminates slightly before on the line $\Omega = \Omega_c$. From the Figures 4.7 and 4.8 it is clear that surface wave modes do not exist for strong magnetic fields.

For a weak dc magnetic field ($\Omega_H = 0.5$) the cutoff frequencies of $S_1^{0.5}$, $S_{-1}^{0.5}$, $S_1^{0.9}$ and $S_{-1}^{0.9}$ in Figures 4.5 and 4.6 are determined by the cutoff curves $TM_{1,1}^{0.5}$, $TM_{-1,1}^{0.5}$, $TM_{1,1}^{0.9}$ and $TM_{-1,1}^{0.9}$ in Figures 4.3 and 4.4 respectively. Hence the occurence of surface wave modes mainly depends on Ω_H, q and S_o. These modes exist only for frequencies above Ω_c and their cutoff's are determined by TE or TM cutoff curves. Generally the lowest of TE or TM cutoff curves determine the surface wave modes.

Now concerning volume modes, for a weak dc magnetic field ($\Omega_H = 0.5$) the volume modes in the exact analysis do not have a common cutoff frequency Ω_c unlike the case of the magnetostatic volume modes as illustrated in (Le-Ngoc,

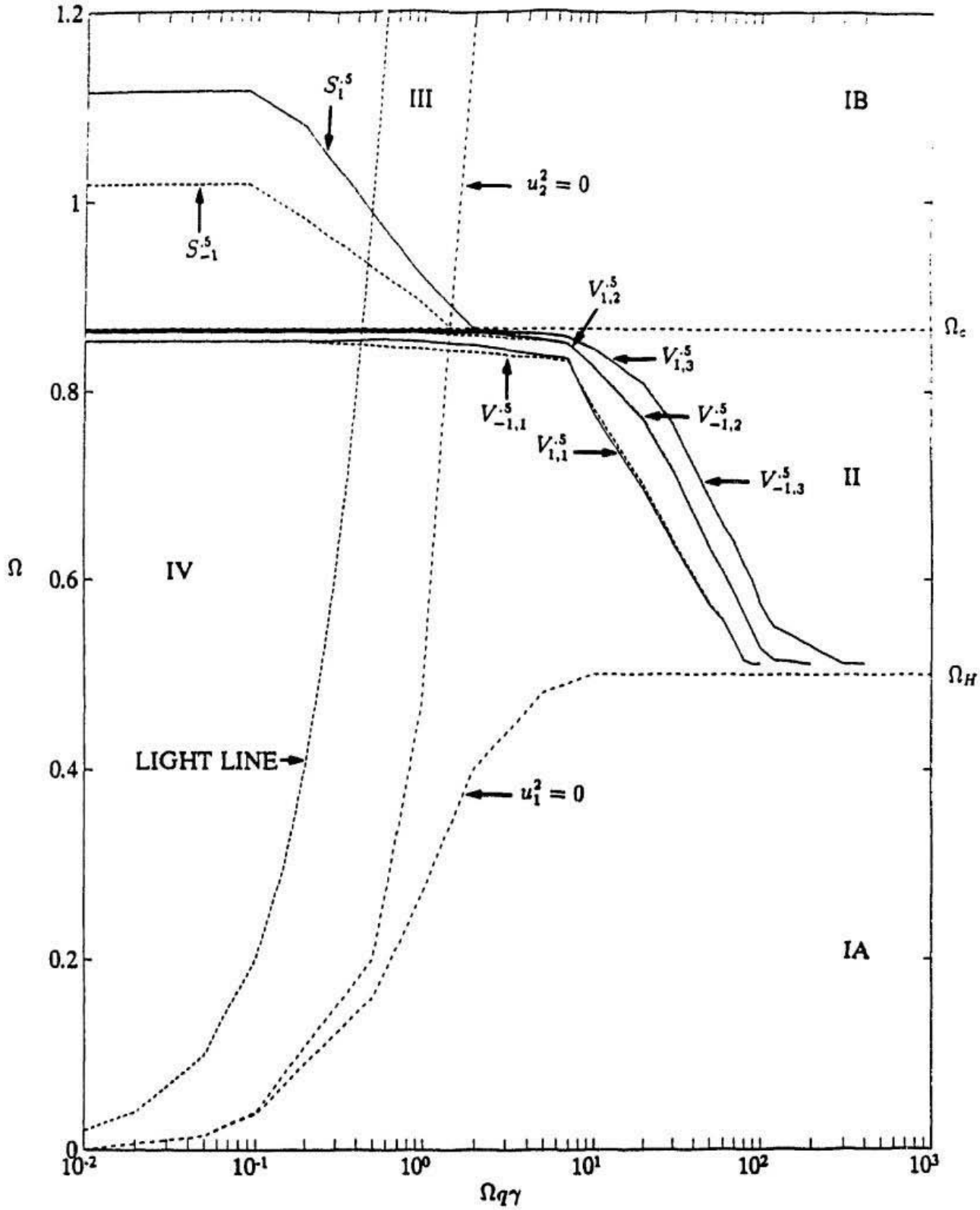

Figure 4.5: Exact dispersion curves for $S_o = 0.5$, $n = \pm 1$, $\Omega_H = 0.5$

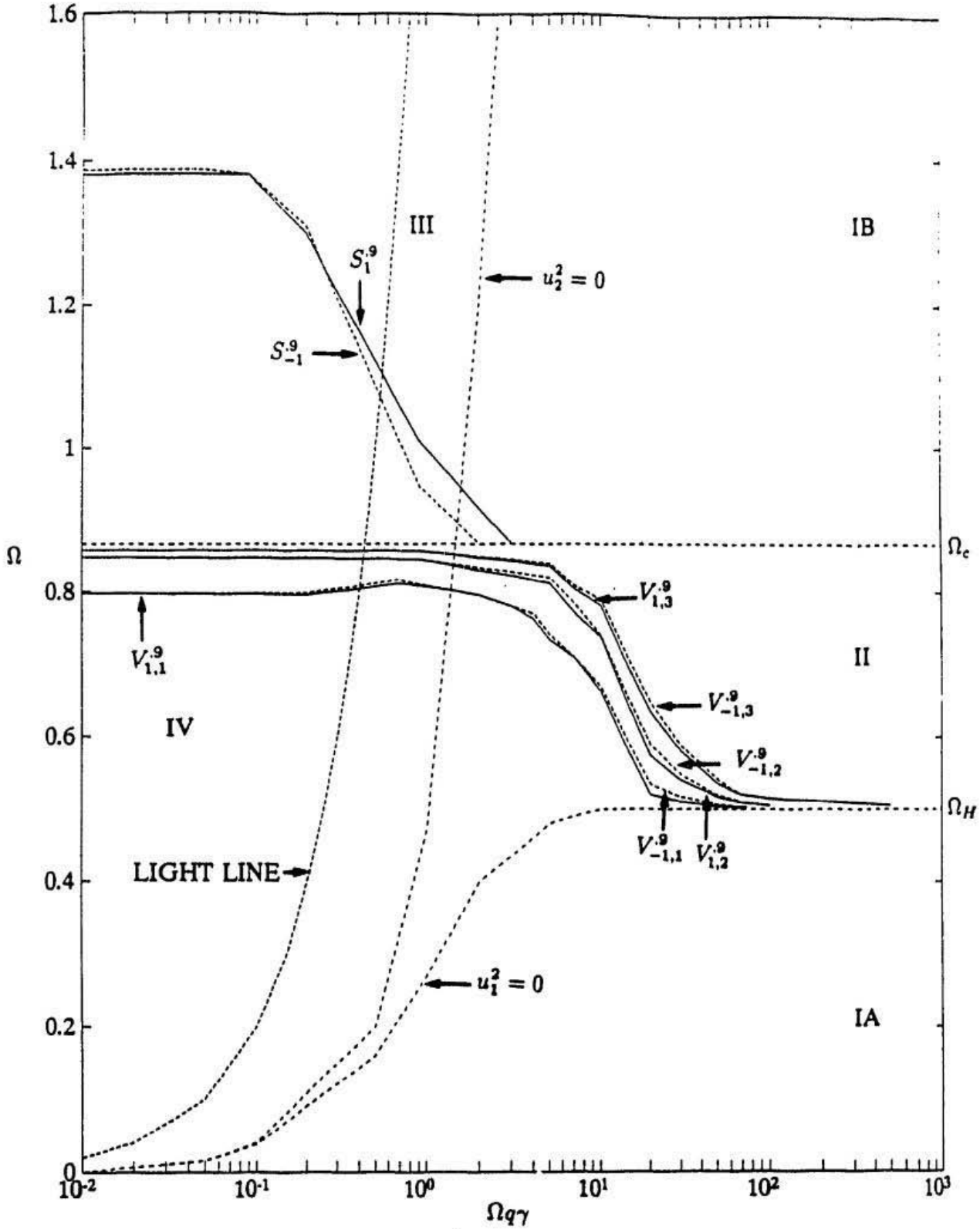

Figure 4.6: Exact dispersion curves for $S_o = 0.9$, $n = \pm 1$, $\Omega_H = 0.5$

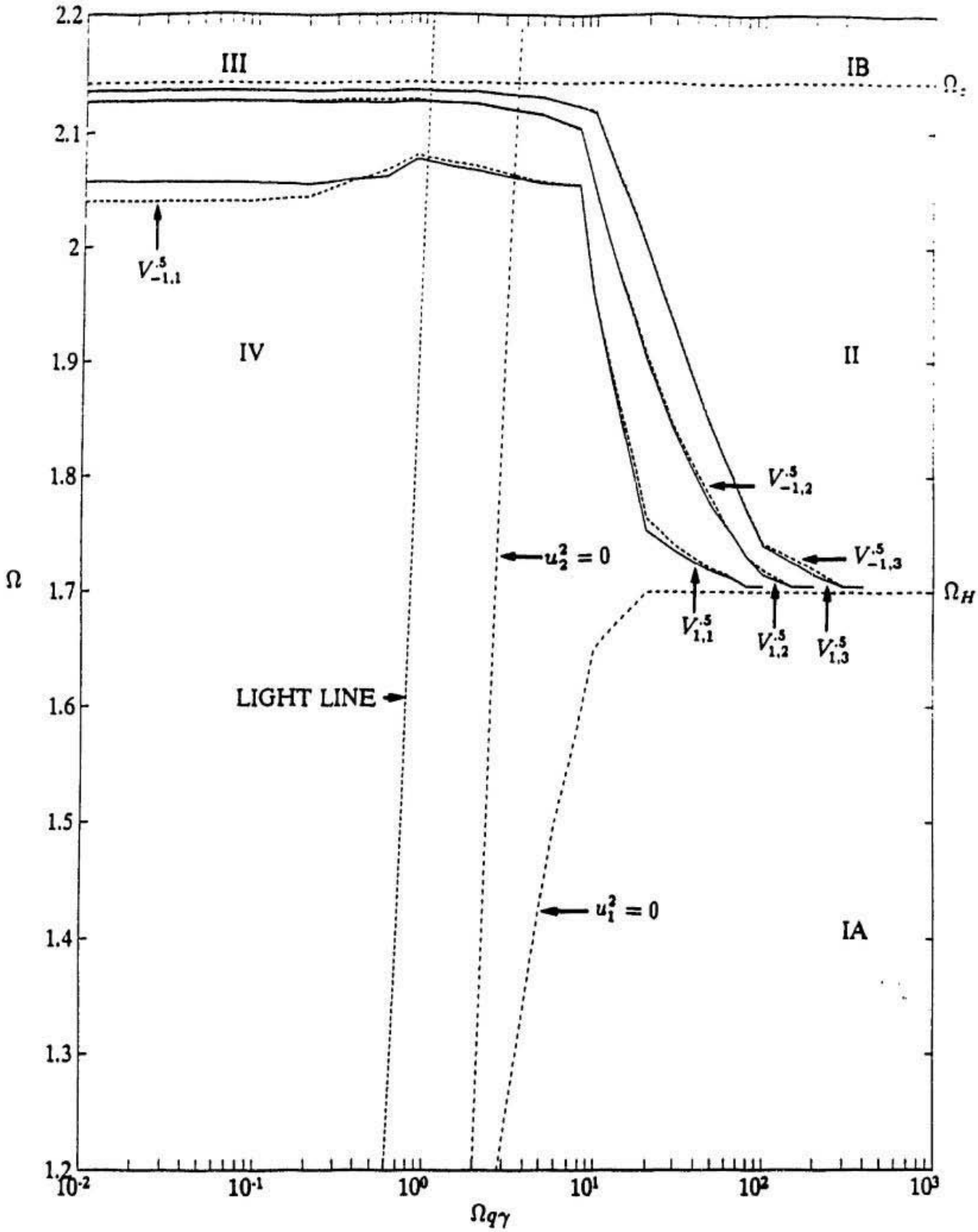

Figure 4.7: Exact dispersion curves for $S_o = 0.5$, $n = \pm 1$, $\Omega_H = 1.7$

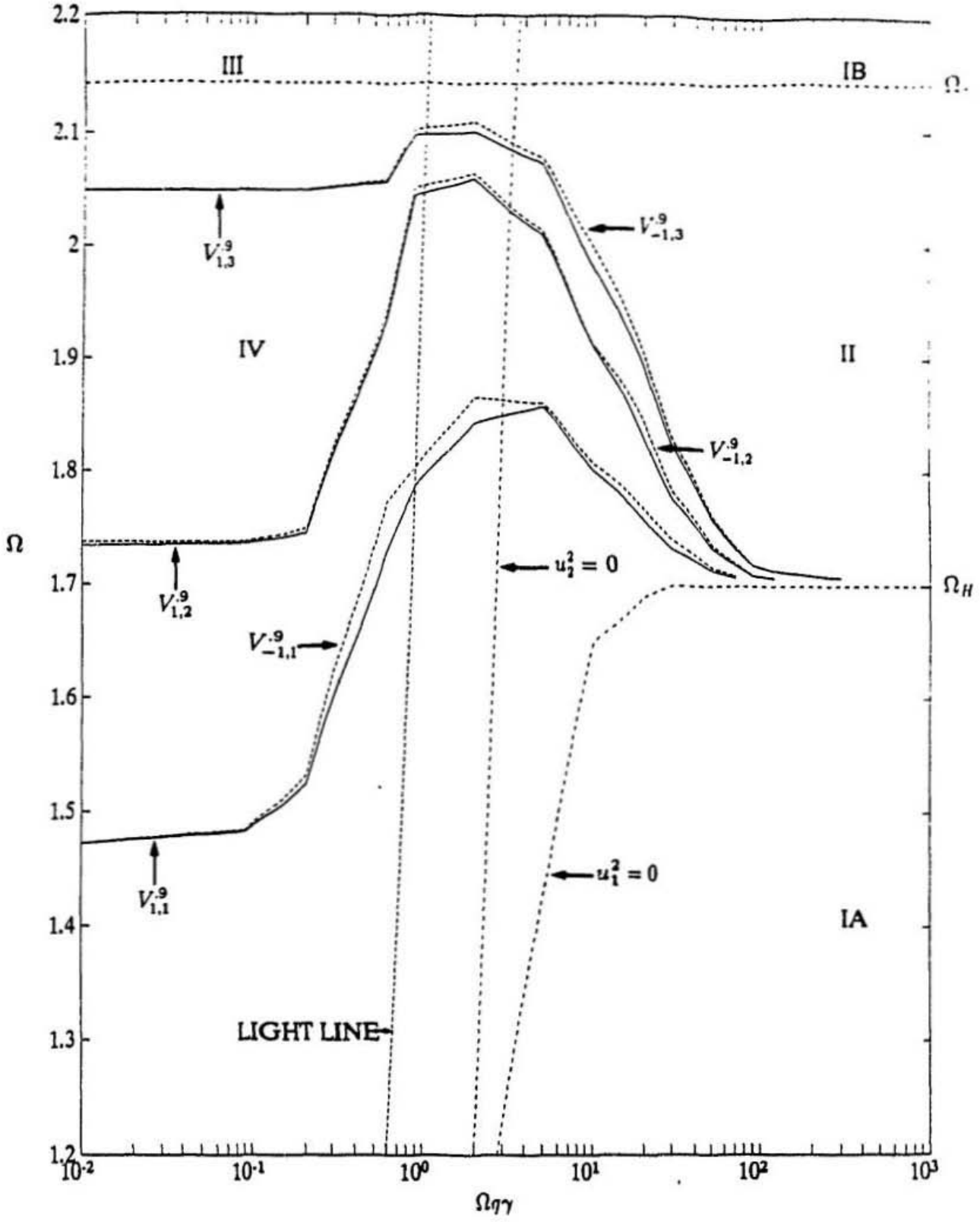

Figure 4.8: Exact dispersion curves for $S_o = 0.9$, $n = \pm 1$, $\Omega_H = 1.7$

1975). For small q, the cutoff frequencies of the TE modes are larger than Ω_c therefore implying that the TE cutoff curves do not determine the cutoff frequencies of the volume modes. The cutoff frequencies of $V_{1,1}^{0.5}$, $V_{1,2}^{0.5}$, $V_{1,3}^{0.5}$, $V_{-1,1}^{0.5}$, $V_{-1,2}^{0.5}$ and $V_{-1,3}^{0.5}$ in Figure 4.5 are determined by the cutoff curves $V_{1,1}^{0.5}$, $V_{1,2}^{0.5}$, $V_{1,3}^{0.5}$, $V_{-1,1}^{0.5}$, $V_{-1,2}^{0.5}$ and $V_{-1,3}^{0.5}$ in Figure 4.3, respectively. Similar behaviour is observed for $S_o = 0.9$, the cutoff frequency of the volume modes in Figure 4.6 are determined by the cutoff curves denoted $V_{n,p}^{S_o}$ in Figure 4.4. For a strong dc magnetic field ($\Omega_H = 1.7$) all the lower order volume modes are forward waves in region IV. The cutoff frequencies of $V_{1,1}^{0.5}$, $V_{1,2}^{0.5}$, $V_{1,3}^{0.5}$, $V_{-1,1}^{0.5}$, $V_{-1,2}^{0.5}$ and $V_{-1,3}^{0.5}$ in Figure 4.7 are determined by the cutoff curves $V_{1,1}^{0.5}$, $V_{1,2}^{0.5}$, $V_{1,3}^{0.5}$ $V_{-1,1}^{0.5}$, $V_{-1,2}^{0.5}$ and $V_{-1,3}^{0.5}$ in Figure 4.3, respectively. The cutoff frequencies of $V_{\pm 1,1}^{0.9}$, $V_{1,2}^{0.9}$, $V_{1,3}^{0.9}$, $V_{-1,2}^{0.9}$ and $V_{-1,3}^{0.9}$ in Figure 4.8 are determined by the cutoff curves $TE_{1,1}^{0.9}$, $V_{1,1}^{0.9}$, $V_{1,2}^{0.9}$, $V_{-1,1}^{0.9}$ and $V_{-1,2}^{0.9}$ in Figure 4.2 and Figure 4.4. A distinct feature of the waves near the line $u_2^2 = 0$ is that they change from forward to backward in Figures 4.7 and 4.8. Thus the dispersion curves for the surface and volume modes are drawn.

The dispersion curves for the modifed waveguide modes are illustrated in Figures 4.9 to 4.12. These modes are not affected to a large extent by variation in Ω_H. The main features of the modified waveguide modes are as follows. As Ω increases the dispersion curves become asymptotic to the normalized phase velocity line (also called light line) especially in the limit of Ω tending to infinity. In general all the dispersion curves of these modes are asymptotic to the line $u_2^2 = 0$ in the limit of $\Omega \to \infty$, the reason being as $\Omega \to \infty$, $u_2^2 \to k_o^2(\epsilon_f - \gamma^2)$ which in turn makes the line $\gamma^2 = \epsilon_f$ coincide with the line $u_2^2 = 0$. For a weak magnetic field the cutoff frequencies of $TM_{1,2}^{0.5}$, $TM_{1,3}^{0.5}$, $TE_{1,1}^{0.5}$, $TE_{1,2}^{0.5}$, $TM_{-1,2}^{0.5}$, $TM_{-1,3}^{0.5}$, $TE_{-1,1}^{0.5}$, and $TE_{-1,2}^{0.5}$ in Figure 4.9 are determined by the cutoff curves $TM_{1,2}^{0.5}$, $TM_{1,3}^{0.5}$, $TE_{1,1}^{0.5}$, $TE_{1,2}^{0.5}$, $TM_{-1,2}^{0.5}$, $TM_{-1,3}^{0.5}$, $TE_{1,1}^{0.5}$, and $TE_{1,2}^{0.5}$ in Figures 4.1 and 4.3. Similarly the cutoff frequencies of $TM_{1,2}^{0.9}$, $TM_{1,3}^{0.9}$, $TE_{1,1}^{0.9}$, $TE_{1,2}^{0.9}$, $TE_{1,3}^{0.9}$, $TM_{-1,2}^{0.9}$, $TM_{-1,3}^{0.9}$, $TE_{-1,1}^{0.9}$, $TE_{-1,2}^{0.9}$

and $TE^{0.9}_{-1,3}$ in Figure 4.10 are determined by the cutoff curves $TM^{0.9}_{1,2}$, $TM^{0.9}_{1,3}$, $TE^{0.9}_{1,1}$, $TE^{0.9}_{1,2}$, $TE^{0.9}_{1,3}$, $TM^{0.9}_{-1,2}$, $TM^{0.9}_{-1,3}$, $TE^{0.9}_{1,1}$, $TE^{0.9}_{1,2}$ and $TE^{0.9}_{1,3}$ in Figures 4.2 and 4.4. For the case of strong magnetic field ($\Omega_H = 1.7$) the cutoff frequencies of $TM^{0.5}_{1,1}$, $TM^{0.5}_{1,2}$, $TM^{0.5}_{1,3}$, $TE^{0.5}_{1,1}$, $TE^{0.5}_{1,2}$, $TM^{0.5}_{-1,1}$, $TM^{0.5}_{-1,2}$, $TM^{0.5}_{1,3}$, $TE^{0.5}_{-1,1}$ and $TE^{0.5}_{-1,2}$ in Figure 4.11 are determined by the cutoff curves $TM^{0.5}_{1,1}$, $TM^{0.5}_{1,2}$, $TM^{0.5}_{1,3}$, $TE^{0.5}_{1,1}$, $TE^{0.5}_{1,2}$, $TM^{0.5}_{-1,1}$, $TM^{0.5}_{-1,2}$, $TM^{0.5}_{-1,3}$, $TE^{0.5}_{1,1}$ and $TE^{0.5}_{1,2}$ in Figures 4.1 and 4.3. Similarly for $S_o = 0.9$, the cutoff frequencies of $TM^{0.9}_{1,1}$, $TM^{0.9}_{1,2}$, $TM^{0.9}_{1,3}$, $TE^{0.9}_{1,2}$, $TE^{0.9}_{1,3}$, $TM^{0.9}_{-1,1}$, $TM^{0.9}_{-1,2}$, $TM^{0.9}_{-1,3}$, $TE^{0.9}_{-1,2}$, $TE^{0.9}_{-1,3}$ in Figure 4.12 are determined by the cutoff curves $TM^{0.9}_{1,1}$, $TM^{0.9}_{1,2}$, $TM^{0.9}_{1,3}$, $TE^{0.9}_{1,2}$, $TE^{0.9}_{1,3}$, $TM^{0.9}_{-1,1}$, $TM^{0.9}_{-1,2}$, $TM^{0.9}_{-1,3}$, $TE^{0.9}_{1,2}$, and $TE^{0.9}_{1,3}$ in Figures 4.2 and 4.4. As can be seen there is no $TE^{0.9}_{\pm 1,1}$ modified waveguide mode present because the cutoff frequency is below Ω_c. Thus the dispersion curves are drawn for the modified waveguide modes.

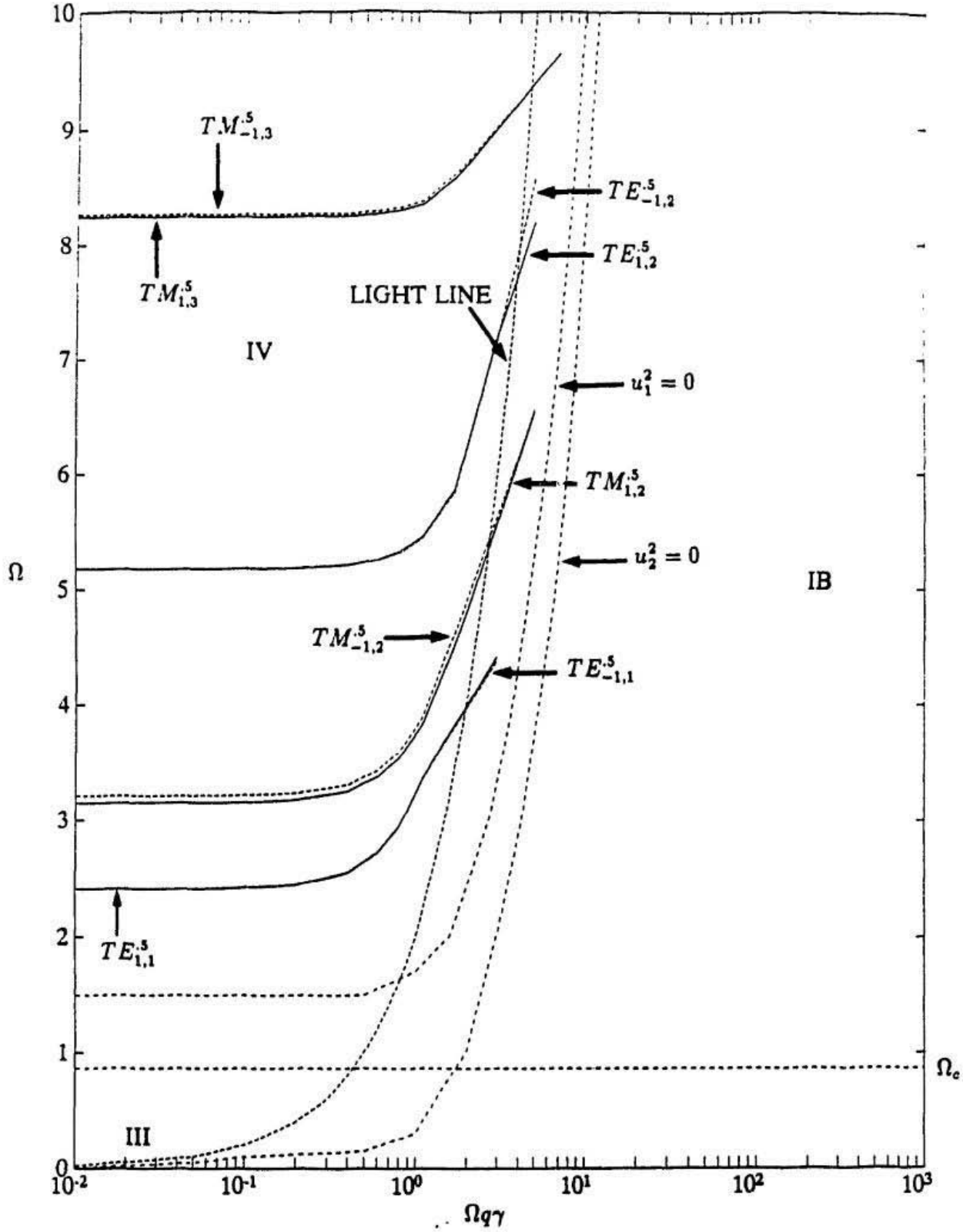

Figure 4.9: Modified waveguide modes for $S_o = 0.5$, $n = \pm 1$, $\Omega_H = 0.5$

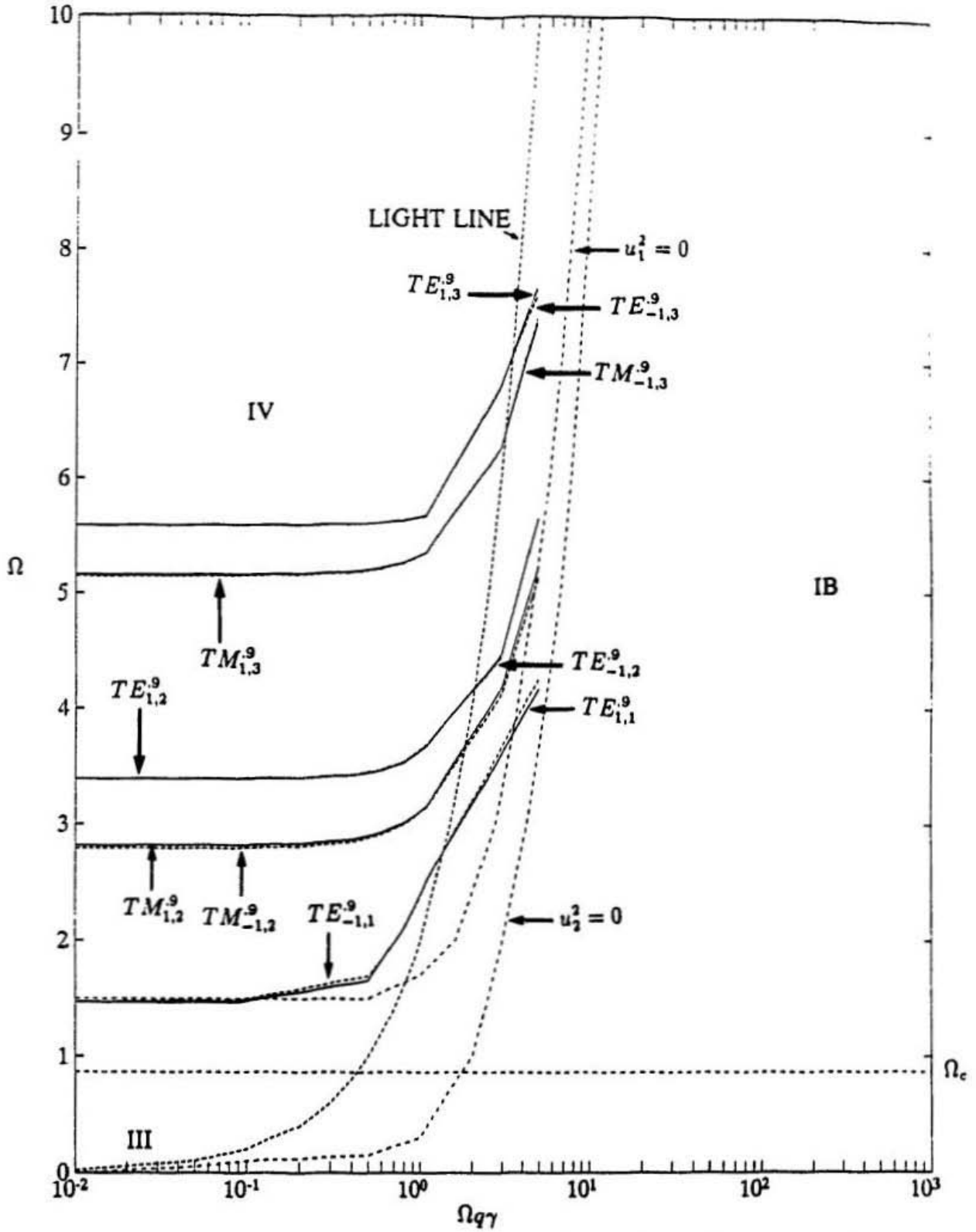

Figure 4.10: Modified waveguide modes for $S_o = 0.9$, $n = \pm 1$, $\Omega_H = 0.5$

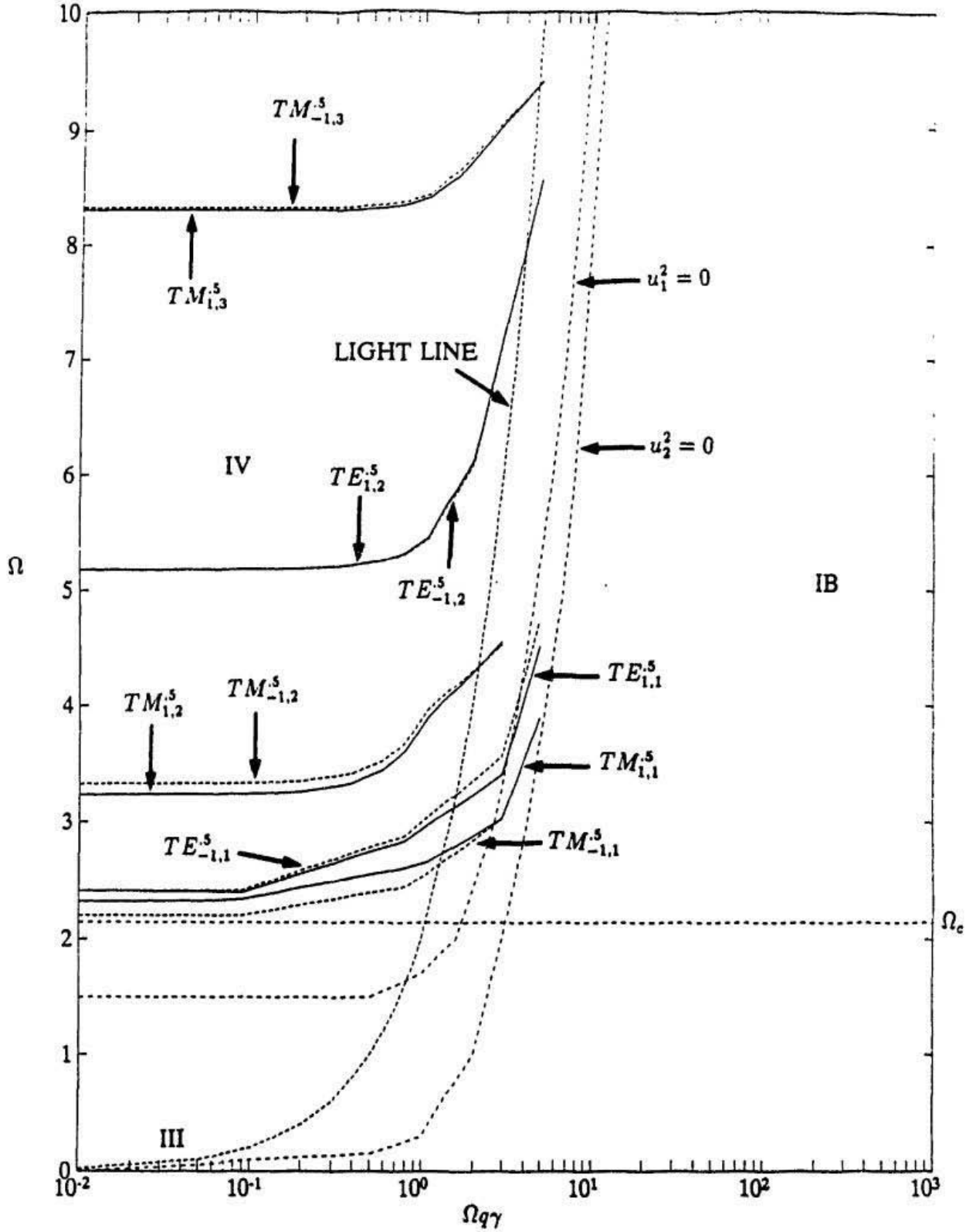

Figure 4.11: Modified waveguide modes for $S_o = 0.5$, $n = \pm 1$, $\Omega_H = 1.7$

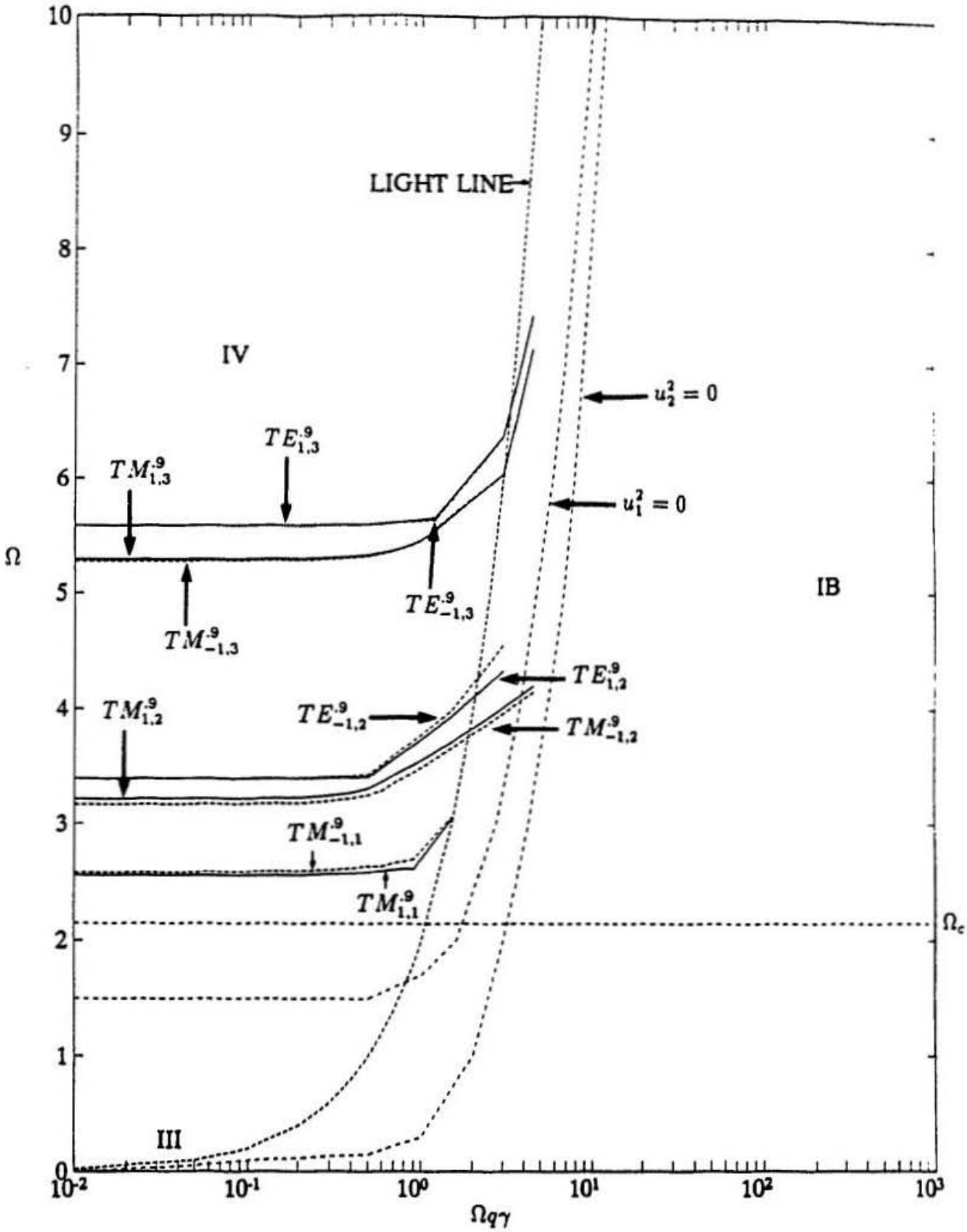

Figure 4.12: Modified waveguide modes for $S_o = 0.9$, $n = \pm 1$, $\Omega_H = 1.7$

Chapter 5

DISCUSSIONS AND CONCLUSIONS

5.1 Applications

The dispersion characteristics and classification of the modes (volume, surface and modified waveguide) were studied in the earlier chapters since they play an important role in some applicational aspects. The results obtained are found to have many applications in microwave devices like gyrators, isolators, circulators and especially phase shifters. In this thesis the applicational aspect with reference to the phase shifter is of main interest. As can be seen from the literature survey, phase shifters loaded with ferrite are found to have applications at microwave and millimeter wave frequencies. The main advantages using ferrites are given as follows:

At a fixed operating frequency, the ferrite parameters are adjusted acccordingly to operate with different types of waves as classified. Another feature is that the permeability tensor of the ferrite can be controlled by varying the dc magnetic field H_o. Also in the ferrite there exists gyroresonance.

Since dipolar modes are considered here the phase velocities are different for $n = 1$ and $n = -1$ modes and thereby implying a possible existence of Faraday rotation. In an earlier study by Le-Ngoc (1980) where a circular waveguide was used, the

Faraday rotation was considerably high for the partially filled ferrite case whereas with the use of a coaxial waveguide the Faraday rotation is considerably low for the partially filled ferrite case ($S_o = 0.5$) and relatively high for the approximately fully filled case ($S_o = 0.9$). But a considerable amount of phase shift is obtained in both the cases. Moreover a detailed study in the phase shift aspect only is considered in this thesis for applicational purposes. Generally the phase shifters are of two types, namely, reciprocal and non-reciprocal. The classification arises depending upon the polarization effects which result in Faraday rotation. For a reciprocal phase shifter there is no Faraday rotation since there is no change in the polarization of the wave transmitted. But for a non-reciprocal phase shifter Faraday rotation exists due to a change in the polarization of the wave that is propagated. By the introduction of ferrite in the waveguide, the Faraday rotation or the phase shift can be changed thereby making it useful in the variable power divider as shown in Figure 5.1 where the direction of power flow is controlled by the change in phase shift produced. The change in phase shift is caused as it depends on the dc magnetic field H_o that is electronically controlled by varying the dc current. The 3 dB coupler divides the power equally and the ground indicated, is in fact a matched load used to prevent any reflection of signal.

In order to obtain an optimal set of dimensions for the design of a variable phase shifter it is necessary to calculate the phase shift in accordance with the operating frequency for which pairs of dominant modified waveguide modes are selected since these modes exhibit phase shift as well as Faraday rotation characteristics. The phase shift produced by a coaxial waveguide loaded with ferrite acts as a variable phase shifter which can be used for rain polarisation compensation similar to the one developed by Le-Ngoc (1980) except that a circular waveguide was used and study of phase shift is done in the Ku band.

The dielectric constant of the ferrite is chosen as 12 and the dielectric constants

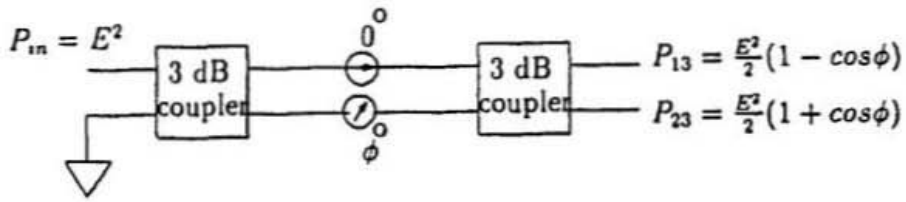

Figure 5.1: Variable power divider

of medium 1 and medium 3 are 2.5 and 1 respectively. The angular saturation magnetization frequency $\omega_m = 25.1327GHz$ and the normalized ferrite column radius $q = \frac{\omega_m d}{v}$ is fixed as 0.5. 'v' being the velocity of light and the radius 'd' calculated to be 0.5968cm which is equal to 0.235". Since $d = 4a$ the value of 'a' is 0.05875". For this data, the dispersion characteristics pertaining to the modified waveguide modes for $n = 1$ and $n = -1$ are determined which are given as follows:

(1) For $S_o = 0.5$, $q = 0.5$ and $\Omega_H = 0.5$, $TE_{\pm 1}$ is the dominant modified waveguide mode

(2) For $S_o = 0.5$, $q = 0.5$ and $\Omega_H = 1.7$, $TE_{\pm 1}$ is the dominant modified waveguide mode

(3) For $S_o = 0.9$, $q = 0.5$ and $\Omega_H = 0.5$, $TE_{\pm 1}$ is the dominant modified waveguide mode

(4) For $S_o = 0.9$, $q = 0.5$ and $\Omega_H = 1.7$, $TM_{\pm 1}$ is the dominant modified waveguide mode

and illustrated in the Figures 5.2 – 5.5, respectively.

Generally the Faraday rotation angle Θ_F and the phase shift Θ_p per unit length

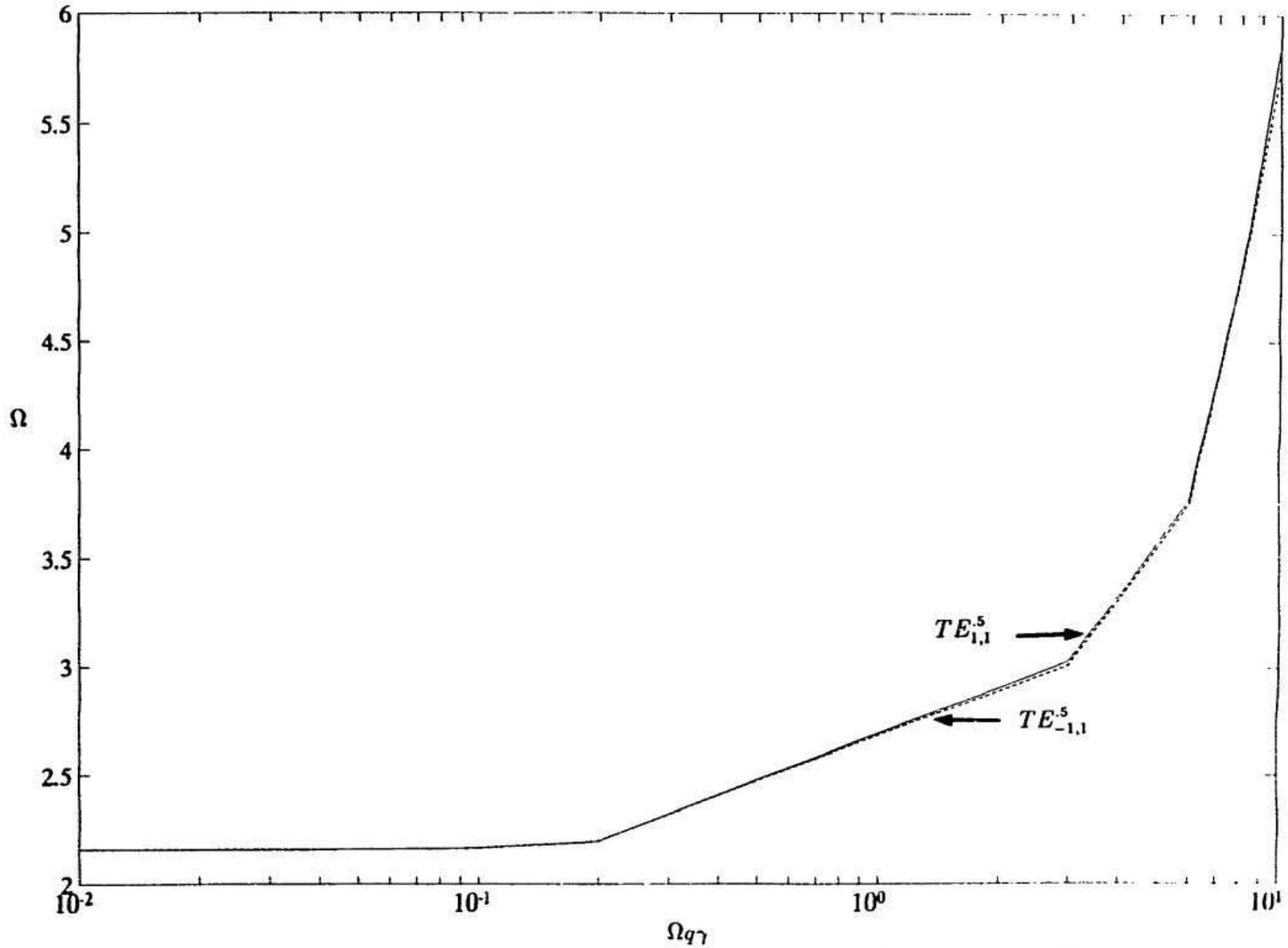

Figure 5.2: A pair of TE dominant modified waveguide modes for $S_o = 0.5$, $q = 0.5$ and $\Omega_H = 0.5$

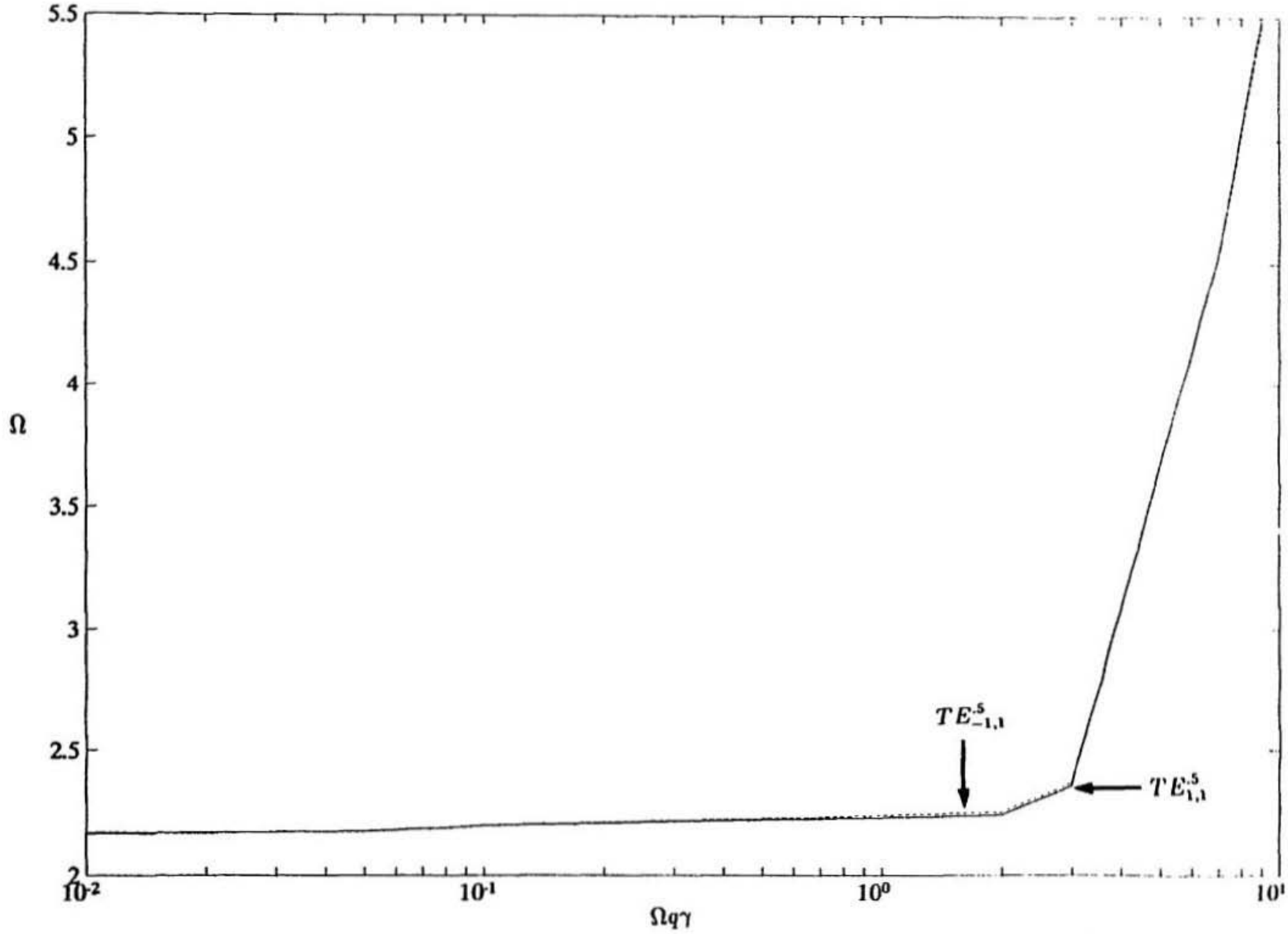

Figure 5.3: A pair of TE dominant modified waveguide modes for $S_c = 0.5$, $q = 0.5$ and $\Omega_H = 1.7$

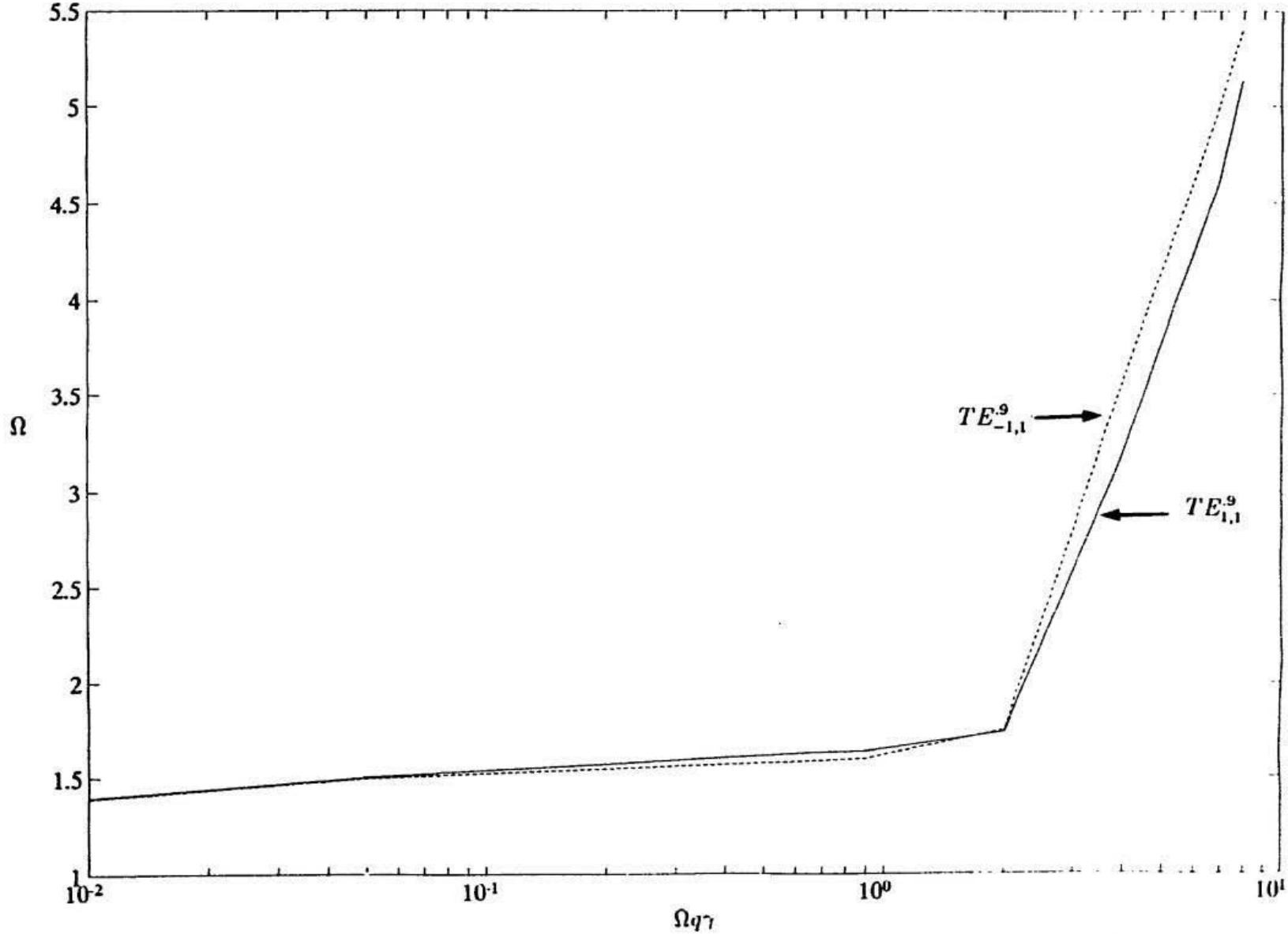

Figure 5.4: A pair of TE dominant modified waveguide modes for $S_\gamma = 0.9$, $q = 0.5$ and $\Omega_H = 0.5$

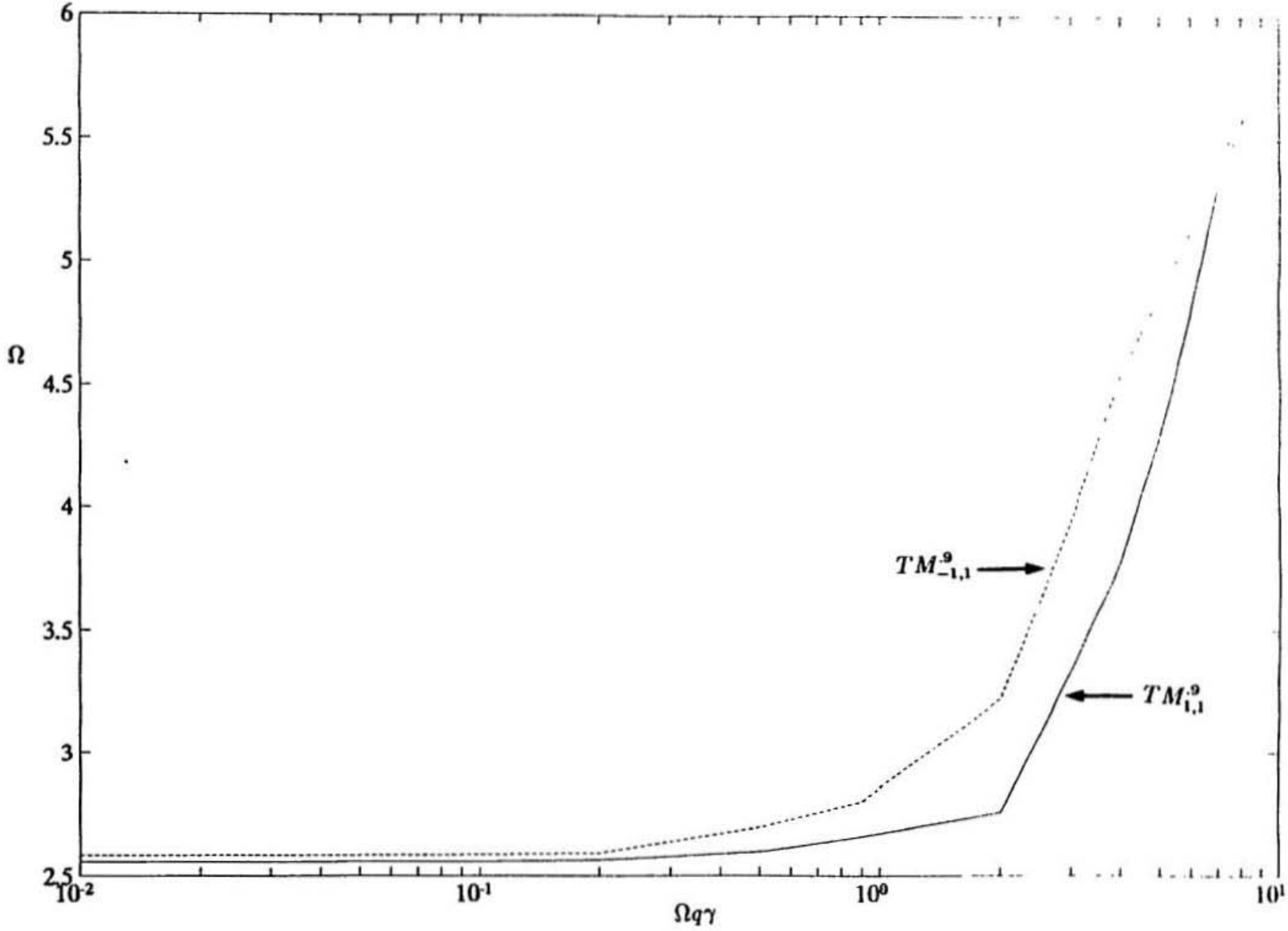

Figure 5.5: A pair of TM dominant modified waveguide modes for $S_w = 0.9$, $q = 0.5$ and $\Omega_H = 1.7$

Table 5.1: Phase shift of $TE_{\pm 1,1}$ dominant modified waveguide modes for $S_o = 0.5$, $q = 0.5$ and $\Omega_H = 0.5$

Normalized frequency Ω	Frequency (GHz)	Phase shift (degrees)
2.75	11	209.4504
3.00	12	469.1689
3.25	13	607.4061
3.50	14	779.1554
3.75	15	955.0938
4.00	16	1055.630

are given by the expressions:

$$\Theta_F = \frac{1}{2}[k^- - k^+] \tag{5.1}$$

and

$$\Theta_p = \frac{1}{2}[k^- + k^+] \tag{5.2}$$

As the dispersion characteristics are plotted between Ω and $\Omega q\gamma$, the expressions for the Faraday rotation and phase shift are rewritten as:

$$\Theta_F = \frac{\Omega q}{2d}[\gamma^- - \gamma^+] \tag{5.3}$$

and

$$\Theta_p = \frac{\Omega q}{2d}[\gamma^- + \gamma^+] \tag{5.4}$$

Now using equation (5.4), the phase shift per unit length for the four cases of the modified waveguide modes are calculated and listed in a tabular form as shown in Tables 5.1 – 5.4. Plots between Phase shift and operating frequency are made for the four cases as shown in the Figures 5.6 – 5.9.

As can be seen from the Figures 5.6 – 5.9 it is clear that the phase shift

Table 5.2: Phase shift of $TE_{\pm 1,1}$ dominant modified waveguide modes for $S_o = 0.5$, $q = 0.5$ and $\Omega_H = 1.7$

Normalized frequency Ω	Frequency (GHz)	Phase shift (degrees)
2.75	11	586.4611
3.00	12	636.7292
3.25	13	720.5093
3.50	14	787.5335
3.75	15	871.3136
4.00	16	955.0938

Table 5.3: Phase shift of $TE_{\pm 1,1}$ dominant modified waveguide modes for $S_o = 0.9$, $q = 0.5$ and $\Omega_H = 0.5$

Normalized frequency Ω	Frequency (GHz)	Phase shift (degrees)
2.75	11	511.0589
3.00	12	578.0831
3.25	13	628.3512
3.50	14	695.3753
3.75	15	770.7774
4.00	16	846.1796

Table 5.4: Phase shift of $TM_{\pm 1,1}$ dominant modified waveguide modes for $S_o = 0.9$, $q = 0.5$ and $\Omega_H = 1.7$

Normalized frequency Ω	Frequency (GHz)	Phase shift (degrees)
2.75	11	206.0992
3.00	12	309.9866
3.25	13	410.5227
3.50	14	473.3579
3.75	15	552.9490
4.00	16	628.3512

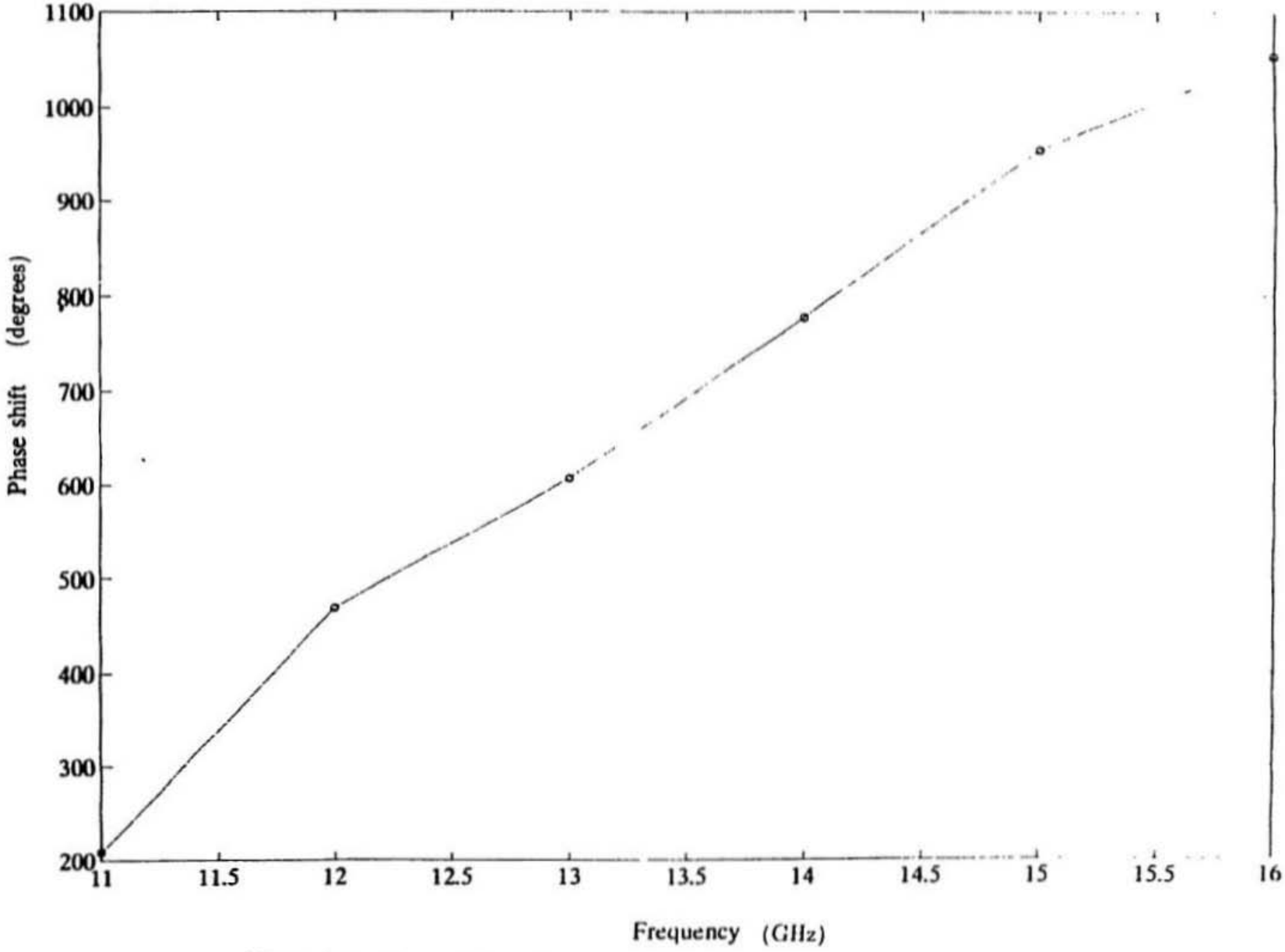

Figure 5.6: Phase shift vs Frequency of $TE_{\pm 1,1}$ dominant modified waveguide modes for $S_o = 0.5$, $q = 0.5$ and $\Omega_H = 0.5$

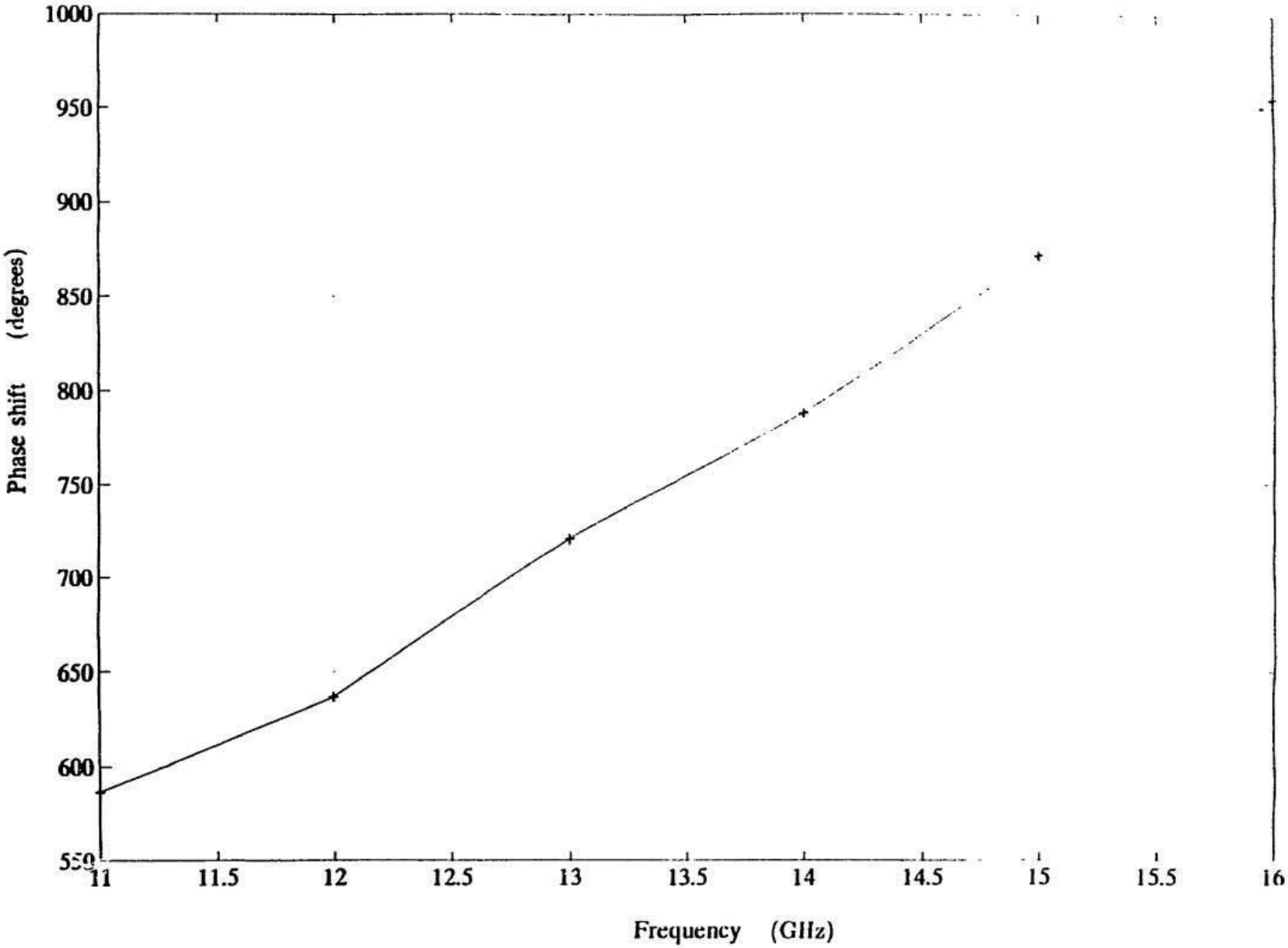

Figure 5.7: Phase shift vs Frequency of $TE_{\pm 1,1}$ dominant modified waveguide modes for $S_o = 0.5$, $q = 0.5$ and $\Omega_H = 1.7$

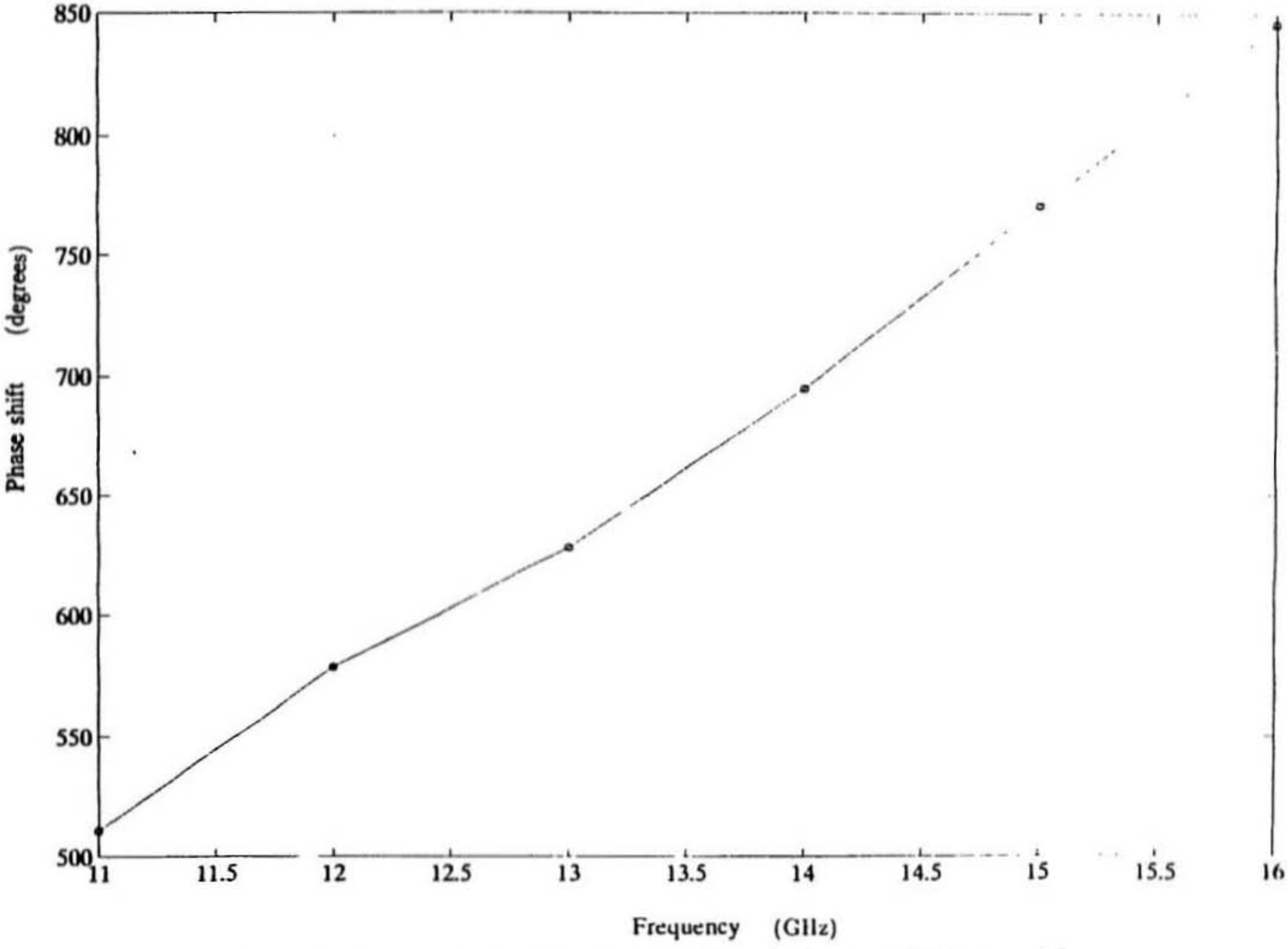

Figure 5.8: Phase shift vs Frequency of $TE_{\pm 1,1}$ dominant modified waveguide modes for $S_o = 0.9$, $q = 0.5$ and $\Omega_H = 0.5$

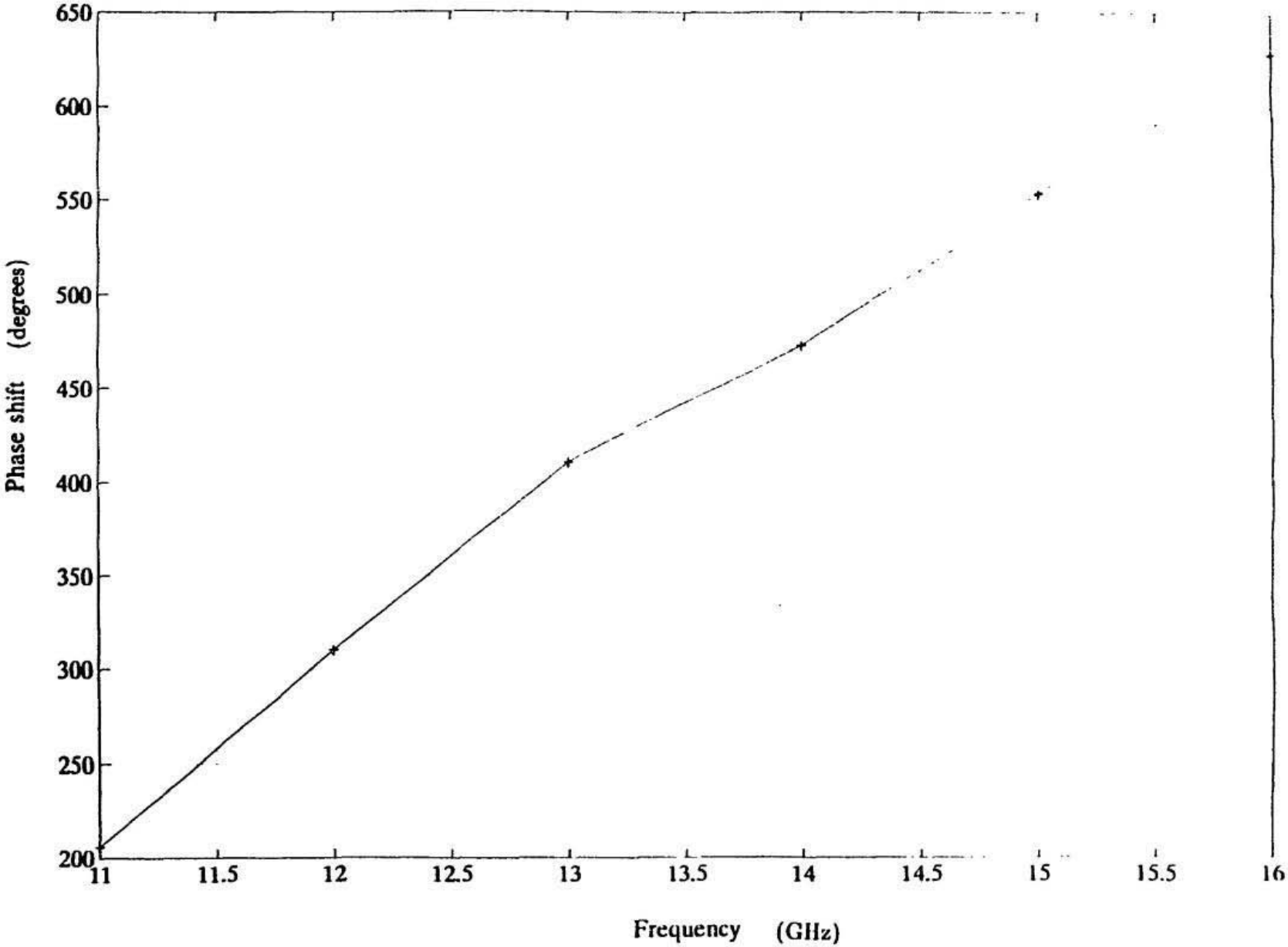

Figure 5.9: Phase shift vs Frequency of $TM_{\pm 1,1}$ dominant modified waveguide modes for $S_o = 0.9$, $q = 0.5$ and $\Omega_H = 1.7$

increases linearly as the frequency increases. Also, it is noted that both Θ_F and Θ_p not only depend on the length but also on the strength of the dc magnetic field applied, therefore they can be electronically controlled by varying the dc current. Thus the coaxial waveguide loaded with ferrite finds applications in phase shifters.

5.2 Conclusions

Electromagnetic wave propagation in a coaxial waveguide loaded with ferrite has been studied for both the partially filled ($S_o = 0.5$) case and the approximately fully filled ($S_o = 0.9$) case by the exact analysis approach. The exact dispersion relations are derived directly from Maxwell's equations. These dispersion relations are first solved for the cutoff and resonant frequencies to predict all possible modes. Then employing the root search technique all points between cutoff and resonance are obtained in order to complete the dispersion curves. The exact analysis is valid for all γ.

The exact field solution modes are hybrid in nature but at cutoff they split up into transverse electric (TE) and transverse magnetic (TM) modes which have been proved analytically. Since both the TE and TM cutoff curves shown in Figures 4.1 - 4.4 determine the cutoff frequencies of the volume modes, these modes are therefore characterized by the transverse electric or transverse magnetic nature at their cutoffs, then change to hybrid nature and finally become transverse electric at resonance. By applying necessary boundary conditions the dispersion relations are obtained. The contributions of this thesis is to gain understanding of the dispersion characteristics of the dipolar modes in a coaxial waveguide loaded with ferrite.

According to the cutoffs and physical characteristics, the modes are classified into three main types, namely, the surface wave modes, volume modes and modified waveguide modes. The surface wave modes not only depend on the dc magnetic field strength Ω_H but also on the radii ratio S_o and the normalized ferrite column radius q . When these parameters are fixed, the occurence of a surface wave mode is established from the TE and TM cutoff curves. This is done by identifying the lowest cutoff frequency among the TE and TM cutoff frequencies which is greater

than the hybrid resonant frequency Ω_c. The suface wave modes exist only in the region where γ is small. These modes start at a cutoff value above Ω_c gradually sloping down and finally terminating on the line $\Omega = \Omega_c$ where its group velocity is zero, thus indicating their backward nature. From the numerical results it is clear that the surface wave modes exist for both $n = 1$ and $n = -1$ cases only for a weak magnetic field. The surface wave modes $S_1^{0.5}$ and $S_1^{0.9}$ are paired with $S_{-1}^{0.5}$ and $S_{-1}^{0.9}$ respectively.

Since the TE cutoff frequencies are larger than Ω_c, the TE cutoff curves do not determine the cutoff frequencies of the volume modes for weak magnetic fields, hence the cutoffs for the volume modes are determined from the TM cutoff curves. These modes exhibit backward nature charateristics. For strong magnetic fields some of the lower order volume modes have their cutoffs determined by the TE cutoff curves. In this case the volume modes are initially forward in nature but gradually change into backward nature near the line $u_2^2 = 0$ or resonance.

The modified waveguide modes are determined by either TE or TM cutoff curves whose frequencies are higher than $\Omega_H + 1$. These modes exhibit both Faraday rotation and phase shift characteristics for the case $S_o = 0.9$ and phase shift characteristics only for the case $S_o = 0.5$. A reciprocal phase shifter can be designed for the coaxial waveguide partially filled with ferrite since there is almost zero Faraday rotation. But for the approximately fully filled ferrite one, a non-reciprocal phase shifter can be designed due to the presence of Faraday rotation. In this thesis, only the phase shift aspect is considered for applications as phase shifter especially in the variable power divider where the power flow is controlled by electronically varying the dc current. The phase shift linearly increases as the frequency is increased and for a given bandwidth the one with a lower frequency

slope is recommended for ideal design.

It is hoped that this work provides an understanding of the propagation of electromagnetic waves in a coaxial waveguide loaded with ferrite for the dipolar modes to the researchers specializing in the area of microwave devices employing anisotropic materials.

REFERENCES

Chiang, K.S. (1991). "Dispersion Characteristics of Strip Dielectric Waveguides", *IEEE Transactions on Microwave Theory and Techniques*, Vol. 39, No. 2, pp. 349-352.

Clarricoats, P.J.B. (1961). *Microwave Ferrites*, John Wiley & Sons Inc., New York, 1st Edition, 260 p.

Collin, R.E. (1966). *Foundations for Microwave Engineering*, McGraw Hill, New York, 589 p.

Daywitt, W.C. (1990). "First-Order Symmetric Modes for a Slightly Lossy Coaxial Transmission Line", *IEEE Transactions on Microwave Theory and Techniques*, Vol. 38, No. 11, pp. 1644-1650.

Duputz, A.M. and Priou, A.C. (1974). "Computer Analysis of Microwave Propagation in a Ferrite Loaded Circular Waveguide - Optimization of Phase-Shifter Longitudinal Field Sections", *IEEE Transactions on Microwave Theory and Techniques*, Vol. MTT-22, No. 6, pp. 601-613.

Fuller, A.J.B. (1987). *Ferrites at Microwave Frequencies*, Peter Peregrinus Ltd., London, United Kingdom, 267 p.

Helszajn, J. (1987). "Architecture of Ferrite Phase Shifters and Control Devices Using Circular Waveguides", *Mikrowellen Military Electronics Magazine*, Vol. 13, No. 1, pp. 70-77.

Igarashi, M. and Nato, Y. (1981). "Parallel Component μ_z of Partially Magnetized Microwave Ferrites", *IEEE Transactions on Microwave Theory and Techniques*, Vol. MTT-29, No. 6, pp. 568-571.

James, G.L. (1983). "Propagation and Radiation Properties of Corrugated Cylindrical Coaxial Waveguides", *IEEE Transactions on Antennas and Propagation*, Vol. AP-31, No. 3, pp. 477-482.

Joseph, R.I. and Schlomann, E. (1961). "Theory of Magnetostatic Modes in Long Axially Magnetized Cylinders", *Journal of Applied Physics*, Vol. 32, No. 6, pp. 1001-1005.

Kales, M.L. (1953). "Modes in Waveguides Containing Ferrites", *Journal of Applied Physics*, Vol. 24, No. 5, pp. 604-608.

Le-Ngoc, S. (1975). "Electromagnetic Wave Propagation in Partially Filled Anisotropic Waveguides", *Ph.D Thesis*, McGill University, Montreal, Quebec, 183 p.

Le-Ngoc, S., Yip, G.L. and Nemoto, S. (1977). "Dispersion Characteristics of the Dipolar Modes in a Waveguide Partially Filled with a Magnetized Ferrite Column", *IEEE Transactions on Microwave Theory and Techniques*, Vol. MTT-25, No. 3, pp. 197-209.

Le-Ngoc, S. (1980). "Phase-shift of the Lossy Ferrite Waveguide used for 12/14 GHz Earth station Polarization tracking",*International Microwave Symposium/Exhibition*, Washington, D.C.

Masuda, M., Chang, N.S. and Matsuo, Y. (1971). "Azimuthally Dependent Magnetostatic Modes in the Cylindrical Ferrites", *IEEE Transactions on Microwave Theory and Techniques*, Vol. MTT-19, No. 10, pp. 834-836.

Mueller, R.S. and Rosenbaum, F.J. (1977). "Propagation along Azimuthally Magnetized Ferrite-Loaded Circular Waveguides", *Journal of Applied Physics*, Vol. 48, No. 6, pp. 2601-2603.

Olson, F.A., Kirchner, E.K., Mehta, K.B., Peternell, F.J. and Morley, B.C. (1967). "Propagation of Magnetostatic Surface Waves in YIG Rods", *Journal of Applied Physics*, Vol. 38, No. 3, pp. 1218-1220.

Samaddar, S.N. (1979). "Special Functions Associated with Azimuthally Magnetized Ferrite Rod Phase Shifters", *Journal of Applied Physics*, Vol. 50, No. 1, pp. 518-520.

Schott, F.W., Tao, T.F. and Freibrun, R.A. (1967). "Electromagnetic Waves in Longitudinally Magnetized Ferrite Rods", *Journal of Applied Physics*, Vol. 38, No. 7, pp. 3015-3022.

Schott, F.W. and Tao, T.F. (1968). "On the Classification of Electromagnetic Waves in Ferrite Rods", *IEEE Transactions on Microwave Theory and Techniques*, Vol. MTT-16, No. 11, pp. 959-961.

Seshadri, S.R. (1973). "Group Velocity Diagrams of a Ferrite Medium", *IEEE Transactions on Antennas and Propagation*, Vol. AP-21, No. 2, pp. 248-250.

Thompson, S.B. and Rodrigue, G.P. (1985). "The Application of Planar Anisotropy to Millimeter-Wave Ferrite Phase Shifters", *IEEE Transactions on Microwave Theory and Techniques*, Vol. MTT-33, No. 11, pp. 1204-1209.

Tompkins, J.E. (1958). "Energy Distribution in Partially Ferrite-Filled Waveguides", *Journal of Applied Physics*, Vol. 29, No. 3, pp. 399-400.

Trivelpiece, A.W., Ignatius, A. and Holscher, P.C. (1961). "Backward Waves in Longitudinally Magnetized Ferrite Rods", *Journal of Applied Physics*, Vol. 32, No. 2, pp. 259-267.